# Spin-wave interaction in two-dimensional ferromagnets with dipolar forces

A. V. Syromyatnikov*
*Petersburg Nuclear Physics Institute, Gatchina, St. Petersburg 188300, Russia*
(Received 1 November 2007; revised manuscript received 3 April 2008; published 30 April 2008)

We discuss the spin-wave interaction in a two-dimensional (2D) Heisenberg ferromagnet (FM) with dipolar forces at $T_C \gg T \geq 0$ by using $1/S$ expansion. A comprehensive analysis is carried out of the first $1/S$ corrections to the spin-wave spectrum. In particular, similar to a three-dimensional FM discussed in our previous paper [A. V. Syromyatnikov, Phys. Rev. B **74**, 014435 (2006)], we show that the spin-wave interaction leads to the *gap* in the spectrum $\epsilon_{\mathbf{k}}$ and greatly renormalizes the bare gapless spectrum at small momenta $k$. The expressions for the spin-wave damping $\Gamma_{\mathbf{k}}$ are derived self-consistently and it is concluded that magnons are *well-defined quasiparticles* in both quantum and classical 2D FMs at small $T$. We observe thermal enhancement of both $\Gamma_{\mathbf{k}}$ and $\Gamma_{\mathbf{k}}/\epsilon_{\mathbf{k}}$ at small momenta. In particular, a peak appears in $\Gamma_{\mathbf{k}}$ and $\Gamma_{\mathbf{k}}/\epsilon_{\mathbf{k}}$ at small $k$ and at any given direction of $\mathbf{k}$. If $S \sim 1$, the height of the peak in $\Gamma_{\mathbf{k}}/\epsilon_{\mathbf{k}}$ is not larger than a value proportional to $T/D \ll 1$, where $D$ is the spin-wave stiffness. In the case of large spins $S \gg 1$, the peak in $\Gamma_{\mathbf{k}}/\epsilon_{\mathbf{k}}$ cannot be greater than that of the classical 2D FM found at $k=0$, the height of which is only *numerically* small: $\Gamma_{\mathbf{0}}/\epsilon_{\mathbf{0}} \approx 0.16$ for the simple square lattice. Frustrating next-nearest-neighbor exchange coupling only slightly increases $\Gamma_{\mathbf{0}}/\epsilon_{\mathbf{0}}$ in a classical 2D FM. We find expressions for spin Green's functions and the magnetization. The latter differs from the well-known result by Maleev [Sov. Phys. JETP **43**, 1240 (1976)]. The effect of the exchange anisotropy is also briefly discussed. Higher order corrections to the spectrum are considered and it is concluded that they are small compared to the first corrections obtained. Our results contradict the findings of previous works [Kashuba *et al.*, Phys. Rev. Lett. **77**, 2554 (1996); Abanov *et al.*, Phys. Rev. B **56**, 3181 (1997)], in which a diffusion spin-wave mode was obtained at small momenta. It is shown that the origin of this discrepancy is that the spin-wave gap was ignored in the previous studies.

DOI: 10.1103/PhysRevB.77.144433 PACS number(s): 75.70.Ak, 75.30.Ds, 75.10.Jm, 75.10.Dg

## I. INTRODUCTION

The magnetic properties of thin films and (quasi-)two-dimensional (2D) magnetic materials are of great interest now.[1,2] This interest is stimulated by recent advances in film growth techniques and numerous technological applications of magnetic films, including uses in electronics and data storage. A realistic theoretical model of low-dimensional magnetic systems must include the exchange interaction, the dipolar interaction, and the magnetocrystalline anisotropy.[1] Despite its smallness, the long-range dipolar interaction plays an essential role in two-dimensional magnets. In particular, it violates the Mermin-Wagner theorem[3] and leads to the stabilization of the long-range magnetic order at finite temperature in 2D magnets.[1,4,5] Some peculiar features have recently been observed at $T \ll T_C$, which are related to the dipolar interaction both in 2D and three-dimensional (3D) Heisenberg ferromagnets (FMs).

In the 3D FM, the problem of infrared singularities arose. It was obtained in Ref. 6 that dipolar forces lead to strong long-wavelength fluctuations, which manifest themselves in an infrared divergence of the first perturbation corrections to the uniform longitudinal spin susceptibility: $\chi_{\|}(\omega \to 0) \sim iT/\omega$. An infrared divergent contribution to the spin-wave stiffness was obtained in Ref. 7 as a result of the analysis of the first $1/S$ corrections to the spin-wave spectrum. Thus, the problem arose of the analysis of the whole perturbation series in order to find the spin-wave spectrum and longitudinal spin susceptibility at small momenta. The appearance of the infrared singularities in these papers is related to the fact that the spectrum is gapless in a 3D FM in the spin-wave approximation.[8]

First perturbation corrections to the spin-wave spectrum were analyzed in a classical 2D FM with dipolar forces in Refs. 9 and 10. It was found that the imaginary part of these corrections exceeds the bare gapless spectrum at small enough momenta $k$. Then, as a result of self-consistent calculations, a diffusion spin-wave mode was obtained at very small $k$. It was argued in Refs. 9 and 10 that despite the analysis is carried out for a classical 2D FM, the diffusion mode should also be observed in a quantum 2D FM.

In the meantime, we find that quite an unusual property of ferromagnets with dipolar forces is ignored in the previous studies, which is crucial for the reported peculiarities—the interaction between magnons leads to the appearance of a *gap* in the spin-wave spectrum that greatly renormalizes the bare gapless spectrum at small momenta. Thus, we obtain such a gap in a 3D FM in the first order of $1/S$ in our recent paper.[11] It was found to be proportional to $\omega_0\sqrt{S\omega_0/J}\sin\theta_{\mathbf{k}}$, where

$$\omega_0 = 4\pi\frac{(g\mu)^2}{v_0} \tag{1}$$

is the characteristic dipolar energy, $v_0$ is the unit cell volume, $\theta_{\mathbf{k}}$ is the angle between momentum $\mathbf{k}$ and the magnetization, and $J$ is the exchange value. We show that this gap screens the infrared singularities obtained in Refs. 6 and 7 and first perturbation corrections to the observables found self-consistently are small. Naturally, one can expect the existence of such a gap in a 2D FM, too.

It should be noted that the appearance of the gap in 2D and 3D FMs is quite expected because a dipolar interaction

 

due to its symmetry and long-range nature violates the Goldstone theorem. Thus, the spin-wave gap was observed in a 2D antiferromagnet with a dipolar interaction in the zeroth order of $1/S$ (i.e., in the spin-wave approximation).[5] The existence of the gap in the spectrum of a 3D FM was anticipated a long time ago. It is well known that within the first order of $1/S$, dipolar and pseudodipolar forces lead to anisotropic corrections to the total energy of a 3D FM.[12–14] As a result, directions along the edges of a cube are energetically favorable in a simple cubic lattice, whereas the magnetization should be parallel to a body diagonal of the cube in a face-centered cubic lattice and a body-centered cubic lattice.[12–15] It has been pointed out by Keffer[14,15] that the anisotropic terms in the total energy of a ferromagnet should be accompanied with an "energy shift" in the spin-wave spectrum. We confirmed this long-standing statement for a 3D FM in our previous paper[11] and demonstrated the relation between the gap and the anisotropy at $T=0$. A fourfold in-plane anisotropy in a square 2D FM caused by quantum fluctuations was also observed before, and the value of this anisotropy was numerically investigated in Ref. 16 for $T \sim SJ$.

The situation is slightly different in classical FMs with a dipolar interaction. In particular, the ground state remains infinitely degenerate according to the rotation about the axis perpendicular to the plane in the classical 2D FM. However, it is well known that in classical systems with degenerate ground states, some of these states can be selected via order-by-disorder mechanism at finite temperature.[17–19] Order-by-disorder effect was demonstrated in 2D systems of classical spins confined to lie within the plane and coupled via (i) a short-range dipolarlike interaction[19] and (ii) long-range dipolar interaction.[20,21] Then, an in-plane anisotropy arises at finite temperature. Notably, it was found in Ref. 21 that the thermal selection of the ground state is accompanied by the appearance of a gap proportional to $T$ in the spin-wave spectrum, which originates from the spin-wave interaction and leads to the finite value of the order parameter. Then, one also expects the appearance of the spin-wave gap in a classical 2D FM with dipolar forces.

In the present paper, we carry out a comprehensive analysis of the first $1/S$ corrections to the spin-wave spectrum in a 2D FM with a dipolar interaction. Similar to a 3D FM, we obtain the spin-wave gap $\Delta$ in the spectrum $\epsilon_{\mathbf{k}}$, which appears to be proportional to $\omega_0\sqrt{S\omega_0/J}$ for $S \sim 1$ and $S\omega_0\sqrt{(\omega_0/J)(T/S^2J)}$ for $S \gg 1$ and $T_C \gg T \gg SJ$. This gap greatly renormalizes the bare gapless spectrum at momenta $k \lesssim [\Delta/(S\omega_0)]^2$. The limiting case of classical spins is also discussed at $T \ll j$ and the gap was found to be proportional to $w\sqrt{Tw/j^2}$, where $j$ and $w$ are values of the exchange and characteristic dipolar energies in the classical model, respectively. It is demonstrated below that the spin-wave gap that was ignored in Refs. 9 and 10 is much larger than the energy of the diffusion mode obtained in those papers. We self-consistently derive the spin-wave damping $\Gamma_{\mathbf{k}}$ and find that spin waves are well-defined quasiparticles in both quantum and classical 2D FMs at small $T$.

Interestingly, we observe a thermal enhancement of the damping at small momenta. In particular, in quantum 2D FMs, we obtain a peak in both $\Gamma_{\mathbf{k}}$ and $\Gamma_{\mathbf{k}}/\epsilon_{\mathbf{k}}$ at $k \ll \omega_0/J$, $T \gg S\omega_0$, and at any given $\mathbf{k}$ direction. If $S \sim 1$, the height of the peak in $\Gamma_{\mathbf{k}}/\epsilon_{\mathbf{k}}$ cannot exceed a value proportional to $T/SJ \ll 1$. In the case of large spins $S \gg 1$, the peak in $\Gamma_{\mathbf{k}}/\epsilon_{\mathbf{k}}$ cannot be greater than that of the classical 2D FM found at $k=0$, the height of which is only *numerically* small: $\Gamma_{\mathbf{0}}/\epsilon_{\mathbf{0}} \approx 0.16$ for the simple square lattice. Frustrating next-nearest-neighbor exchange coupling only slightly increases $\Gamma_{\mathbf{0}}/\epsilon_{\mathbf{0}}$ in classical 2D FMs.

We derive expressions for spin Green's functions and the magnetization. The latter differs from the well-known result of Ref. 4. The effect of the exchange anisotropy is also briefly discussed. Higher order corrections to the spectrum are considered and it is concluded that they are small compared to the first corrections obtained. We derive the fourfold in-plain anisotropy in the total energy of quantum 2D FMs that makes the directions of the magnetization along the edges of the square to be energetically favorable in the simple square lattice. We also demonstrate the relation between this anisotropy and the spin-wave gap at $T=0$ as was done in our previous paper[11] for 3D FMs. The spin-wave interaction in 2D FMs with a small number of layers and with dipolar forces was numerically discussed in Ref. 22.

The rest of the present paper is organized as follows. The Hamiltonian transformation and the technique are discussed in Sec. II. First $1/S$ corrections to the real and imaginary parts of the spin-wave spectrum are considered in Secs. III and IV, respectively. In Sec. V, we study the case of large spin values and consider the limit of classical spins. In Sec. VI, we (i) demonstrate the relation between the anisotropic term in the total energy appearing due to the dipolar interaction and the spin-wave gap at $T=0$, (ii) discuss the further order $1/S$ corrections to the spin-wave spectrum, (iii) calculate the magnetization by taking into account the spin-wave spectrum renormalization, (iv) derive the spin Green's functions in the first order of $1/S$, and (v) briefly discuss the effect of the easy-plane anisotropy and consider the spectrum renormalization obtained in Refs. 9 and 10. Section VII contains a detailed summary and our conclusion. Three appendixes are included with some details of calculations.

## II. HAMILTONIAN TRANSFORMATION AND TECHNIQUE

The Hamiltonian of a ferromagnet with dipolar interaction has the form

$$\mathcal{H} = -\frac{1}{2}\sum_{l \neq m} (J_{lm}\delta_{\rho\beta} + Q_{lm}^{\rho\beta}) S_l^{\rho} S_m^{\beta}, \tag{2}$$

$$Q_{lm}^{\rho\beta} = (g\mu)^2 \frac{3R_{lm}^{\rho}R_{lm}^{\beta} - \delta_{\rho\beta}R_{lm}^2}{R_{lm}^5}. \tag{3}$$

By taking the Fourier transformation, we have from Eq. (2)

$$\mathcal{H} = -\frac{1}{2}\sum_{\mathbf{k}} (J_{\mathbf{k}}\delta_{\rho\beta} + Q_{\mathbf{k}}^{\rho\beta}) S_{\mathbf{k}}^{\rho} S_{-\mathbf{k}}^{\beta}, \tag{4}$$

where $J_{\mathbf{k}} = \Sigma_l J_{lm} \exp(i\mathbf{k}\mathbf{R}_{lm})$ and $Q_{\mathbf{k}}^{\rho\beta} = \Sigma_l Q_{lm}^{\rho\beta} \exp(i\mathbf{k}\mathbf{R}_{lm})$. We direct the $y$ axis perpendicular to the lattice, as is shown in Fig. 1. The dipolar tensor $Q_{\mathbf{k}}^{\rho\beta}$ possesses the following well-

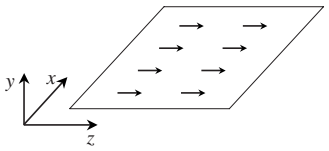


FIG. 1. Two-dimensional ferromagnet discussed in the present paper.

known properties[1,4] at $k \ll 1$, which are independent of the lattice type and the orientation of $x$ and $z$ axes relative to the lattice:

$$Q_{\mathbf{k}}^{\rho\beta} = \omega_0 \left( \frac{\alpha}{3} \delta_{\rho\beta} - \frac{k}{2} \frac{k_\rho k_\beta}{k^2} \right), \quad \text{where} \quad \rho, \beta = x, z, \tag{5}$$

$$Q_{\mathbf{k}}^{y\beta} = \omega_0 \left( -\frac{2}{3}\alpha + \frac{k}{2} \right) \delta_{y\beta}, \quad \text{where} \quad \beta = x, y, z, \tag{6}$$

$$\alpha = \frac{3v_0}{8\pi} \sum_i \frac{1}{R_i^3}, \tag{7}$$

where we set the lattice spacing to be equal to unity, $\omega_0$ is the characteristic dipolar energy given by Eq. (1), and $\alpha$ is a constant that is approximately equal to 1.078 for the simple square lattice. It is seen from Eqs. (2), (5), and (6) that dipolar forces lead to an easy-plane anisotropy in the energy of the classical 2D FM with $y$ being a hard axis.[4] We show in Sec. III that quantum and thermal fluctuations also lead to an in-plane anisotropy. We direct the $z$ axis along the uniform magnetization, as shown in Fig. 1.

After Dyson–Maleev transformation,[8,23–25]

$$S_{\mathbf{k}}^x = \sqrt{\frac{S}{2}} \left( a_{\mathbf{k}} + a_{-\mathbf{k}}^\dagger - \frac{(a^\dagger a^2)_{\mathbf{k}}}{2S} \right),$$

$$S_{\mathbf{k}}^y = -i\sqrt{\frac{S}{2}} \left( a_{\mathbf{k}} - a_{-\mathbf{k}}^\dagger - \frac{(a^\dagger a^2)_{\mathbf{k}}}{2S} \right), \quad S_{\mathbf{k}}^z = S - (a^\dagger a)_{\mathbf{k}}. \tag{8}$$

Hamiltonian (4) has the form $\mathcal{H} = E_0 + \Sigma_{i=1}^6 \mathcal{H}_i$, where $E_0$ is the ground state energy and $\mathcal{H}_i$ denote terms containing products of $i$ operators $a$ and $a^\dagger$. One should take into account terms up to $\mathcal{H}_4$ to calculate corrections of the first order in $1/S$. $\mathcal{H}_1 = 0$ because it contains only $Q_{\mathbf{0}}^{\rho\beta}$ with $\rho \neq \beta$. For the remaining necessary terms, one has

$$\mathcal{H}_2 = \sum_{\mathbf{k}} \left[ E_{\mathbf{k}} a_{\mathbf{k}}^\dagger a_{\mathbf{k}} + \frac{B_{\mathbf{k}}}{2} (a_{\mathbf{k}} a_{-\mathbf{k}} + a_{\mathbf{k}}^\dagger a_{-\mathbf{k}}^\dagger) \right], \tag{9}$$

$$\mathcal{H}_3 = \sqrt{\frac{S}{2\mathfrak{N}}} \sum_{\mathbf{k}_1+\mathbf{k}_2+\mathbf{k}_3=\mathbf{0}} Q_2^{xz} a_{-1}^\dagger (a_{-2}^\dagger + a_2) a_3, \tag{10}$$

$$\mathcal{H}_4 = \frac{1}{4\mathfrak{N}} \sum_{\mathbf{k}_1+\mathbf{k}_2+\mathbf{k}_3+\mathbf{k}_4=\mathbf{0}} \{ 2(J_1 - J_{1+3}) a_{-1}^\dagger a_{-2}^\dagger a_3 a_4 + a_{-1}^\dagger [ a_2 (Q_2^{xx} - Q_2^{yy}) + a_{-2}^\dagger (Q_2^{xx} + Q_2^{yy} - 2Q_{2+3}^{zz}) ] a_3 a_4 \}, \tag{11}$$

where we drop index $\mathbf{k}$ in Eqs. (10) and (11), $\mathfrak{N}$ is the number of spins in the lattice, and

$$E_{\mathbf{k}} = S(J_0 - J_{\mathbf{k}}) - \frac{S}{2} \left( Q_{\mathbf{k}}^{xx} + Q_{\mathbf{k}}^{yy} - \frac{2\omega_0\alpha}{3} \right)$$
$$\overset{k\ll 1}{\approx} Dk^2 + \frac{S\omega_0\alpha}{2} - \frac{S\omega_0}{4} k \cos^2 \phi_{\mathbf{k}}, \tag{12}$$

$$B_{\mathbf{k}} = \frac{S}{2}(Q_{\mathbf{k}}^{yy} - Q_{\mathbf{k}}^{xx}) \overset{k\ll 1}{\approx} -\frac{S\omega_0\alpha}{2} + \frac{S\omega_0}{4} k (1 + \sin^2 \phi_{\mathbf{k}}), \tag{13}$$

where $D$ is the spin-wave stiffness, $\phi_{\mathbf{k}}$ is the angle between $\mathbf{k}$ and the magnetization, and the expressions after $\overset{k\ll 1}{\approx}$ are approximate values of the corresponding quantities at $k \ll 1$. For the coupling between only nearest-neighbor spins on the simple square lattice, one has $D = SJ$. In the spin-wave approximation, for the magnon spectrum, we find

$$\epsilon_{\mathbf{k}} = \sqrt{E_{\mathbf{k}}^2 - B_{\mathbf{k}}^2} \overset{k\ll 1}{\approx} \sqrt{(Dk^2 + S\omega_0\alpha) \left( Dk^2 + \frac{S\omega_0}{2} k \sin^2 \phi_{\mathbf{k}} \right)}, \tag{14}$$

which is in accordance with the well-known result.[4]

To perform the calculations, it is convenient to introduce the following retarded Green's functions: $G(\omega, \mathbf{k}) = \langle a_{\mathbf{k}}, a_{\mathbf{k}}^\dagger \rangle_\omega$, $F(\omega, \mathbf{k}) = \langle a_{\mathbf{k}}, a_{-\mathbf{k}} \rangle_\omega$, $\bar{G}(\omega, \mathbf{k}) = \langle a_{-\mathbf{k}}^\dagger, a_{-\mathbf{k}} \rangle_\omega = G^*(-\omega, -\mathbf{k})$, and $F^\dagger(\omega, \mathbf{k}) = \langle a_{-\mathbf{k}}^\dagger, a_{\mathbf{k}}^\dagger \rangle_\omega = F^*(-\omega, -\mathbf{k})$. We have two sets of Dyson equations for them. One of these sets has the form

$$G(\omega, \mathbf{k}) = G^{(0)}(\omega, \mathbf{k}) + G^{(0)}(\omega, \mathbf{k}) \bar{\Sigma}(\omega, \mathbf{k}) G(\omega, \mathbf{k}) + G^{(0)}(\omega, \mathbf{k}) \times [B_{\mathbf{k}} + \Pi(\omega, \mathbf{k})] F^\dagger(\omega, \mathbf{k}),$$

$$F^\dagger(\omega, \mathbf{k}) = \bar{G}^{(0)}(\omega, \mathbf{k}) \Sigma(\omega, \mathbf{k}) F^\dagger(\omega, \mathbf{k}) + \bar{G}^{(0)}(\omega, \mathbf{k}) [B_{\mathbf{k}} + \Pi^\dagger(\omega, \mathbf{k})] G(\omega, \mathbf{k}), \tag{15}$$

where $G^{(0)}(\omega, \mathbf{k}) = (\omega - E_{\mathbf{k}} + i\delta)^{-1}$ is the bare Green's function and $\Sigma$, $\bar{\Sigma}$, $\Pi$, and $\Pi^\dagger$ are the self-energy parts. By solving Eq. (15), one obtains

$$G(\omega, \mathbf{k}) = \frac{\omega + E_{\mathbf{k}} + \Sigma(\omega, \mathbf{k})}{\mathcal{D}(\omega, \mathbf{k})},$$

$$F(\omega, \mathbf{k}) = -\frac{B_{\mathbf{k}} + \Pi(\omega, \mathbf{k})}{\mathcal{D}(\omega, \mathbf{k})},$$

$$\bar{G}(\omega, \mathbf{k}) = \frac{-\omega + E_{\mathbf{k}} + \bar{\Sigma}(\omega, \mathbf{k})}{\mathcal{D}(\omega, \mathbf{k})},$$

$$F^\dagger(\omega, \mathbf{k}) = -\frac{B_{\mathbf{k}} + \Pi^\dagger(\omega, \mathbf{k})}{\mathcal{D}(\omega, \mathbf{k})}, \tag{16}$$

where

$$\mathcal{D}(\omega, \mathbf{k}) = (\omega + i\delta)^2 - \epsilon_{\mathbf{k}}^2 - \Omega(\omega, \mathbf{k}), \tag{17}$$

$$\Omega(\omega,\mathbf{k}) = E_{\mathbf{k}}(\Sigma + \bar{\Sigma}) - B_{\mathbf{k}}(\Pi + \Pi^{\dagger}) - (\omega + i\delta)(\Sigma - \bar{\Sigma}) - \Pi\Pi^{\dagger} + \Sigma\bar{\Sigma}, \tag{18}$$

and $\epsilon_{\mathbf{k}}$ is given by Eq. (14). The quantity $\Omega(\omega,\mathbf{k})$ given by Eq. (18) describes renormalization of the spin-wave spectrum square. We calculate the real part of $\Omega(\omega,\mathbf{k})$ in Sec. III and analyze its imaginary part in Sec. IV. The last two terms in Eq. (18) give the corrections of at least second order in $1/S$ and are not considered in Secs. III–V. We imply that $S \sim 1$ in Secs. III and IV, and discuss large $S$ in Sec. V.

## III. RENORMALIZATION OF THE REAL PART OF THE SPIN-WAVE SPECTRUM

The corrections to the spin-wave spectrum to be obtained are proportional to sums over momenta in which summands depend on the components of the dipolar tensor $Q_{\mathbf{k}}^{\rho\beta}$. In some of these sums, a summation over small momenta is important and one can use expressions (5) and (6) for $Q_{\mathbf{k}}^{\rho\beta}$. In the meantime, there are sums in which a summation over large momenta is essential and which, consequently, depend on the direction of the quantized axis within the plane and the lattice type. Thus, one should bear in mind what the direction of the magnetization in the ground state is.

Therefore, the well-known fact that dipolar and pseudodipolar interactions lead to the dependence of the energy of a ferromagnet on the direction of quantized axis should be taken into account.[12,14] We now show that, being established first for 3D FMs, this finding also remains valid for 2D FMs: apart from the easy-plane anisotropy found in Ref. 4 and discussed above, there is also an in-plane anisotropy. As in 3D FMs, the first $1/S$ correction to the classical energy $E_0$ having the form

$$\Delta E = \langle \mathcal{H}_2 \rangle = \sum_{\mathbf{k}} \frac{\epsilon_{\mathbf{k}} - E_{\mathbf{k}}}{2} \approx -\sum_{\mathbf{k}} \frac{B_{\mathbf{k}}^2}{2(\epsilon_{\mathbf{k}} + E_{\mathbf{k}})} \tag{19}$$

gives rise to such an in-plane anisotropy, wherein the isotropic term is omitted in the right part of Eq. (19). After direct calculations, for a square lattice, one obtains

$$\frac{\Delta E}{\mathfrak{N}} = C\frac{(S\omega_0)^2}{2D}\gamma_x^2\gamma_z^2, \tag{20}$$

$$C = \frac{D}{\omega_0^2\mathfrak{N}}\sum_{\mathbf{q}} \frac{(Q_{\mathbf{q}}^{xx} - Q_{\mathbf{q}}^{zz})^2 - 4(Q_{\mathbf{q}}^{xz})^2}{8\epsilon_{\mathbf{q}}}, \tag{21}$$

where $\gamma_i$ are direction cosines of the magnetization, and components of the dipolar tensor in Eq. (21) are taken relative to square axes. The constant $C$ should be numerically calculated because the summation over large momenta is important in Eq. (21) and one cannot use Eqs. (5) and (6) for the dipolar tensor components. This calculation can be carried out by using the dipolar sums computation technique (see, e.g., Ref. 26 and references therein) with the result $C \approx 0.0082$ for exchange coupling only between nearest-neighbor spins on the simple square lattice. Because $C > 0$, an edge of the square is the easy direction. Notice also that the value of the dipolar anisotropy in a cubic 3D FM is proportional to a constant that also has the form (21), wherein, naturally, summation is taken over 3D reciprocal vectors.[11] The in-plane anisotropy caused by a dipolar interaction was numerically investigated at $T \sim D$ in Ref. 16.

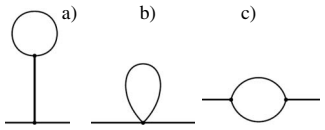


FIG. 2. Diagrams of the first order in $1/S$ for self-energy parts discussed in this paper. Diagrams (a) and (c) stem from three-magnon terms (10) in the Hamiltonian, whereas (b) comes from four-magnon terms (11).

We now study separately the bubble diagrams shown in Figs. 2(a) and 2(b), and the loop diagram presented in Fig. 2(c).

### A. Bubble diagrams

Let us start with the diagram shown in Fig. 2(a). It appears from three-magnon terms (10) and gives a value of zero. To demonstrate this, we make all possible couplings of two operators $a$ and $a^{\dagger}$ in Eq. (10), as follows:

$$(a_0^{\dagger} + a_0)\sqrt{\frac{S}{2\mathfrak{N}}}\sum_{\mathbf{q}} \frac{(E_{\mathbf{q}} - B_{\mathbf{q}})(1 + 2N_{\mathbf{q}}) - \epsilon_{\mathbf{q}}}{2\epsilon_{\mathbf{q}}} Q_{\mathbf{q}}^{xz}, \tag{22}$$

where $N_{\mathbf{q}} = (e^{\epsilon_{\mathbf{q}}/T} - 1)^{-1}$ is Plank's function. Expression (22) is equal to zero because $Q_{\mathbf{q}}^{xz} = -Q_{\mathbf{q}'}^{xz}$, $E_{\mathbf{q}} = E_{\mathbf{q}'}$, and $B_{\mathbf{q}} = B_{\mathbf{q}'}$, where $\mathbf{q} = (q_x, q_z)$ and $\mathbf{q}' = (-q_x, q_z)$.

The Hartree–Fock diagram presented in Fig. 2(b) comes from $\mathcal{H}_4$ terms given by Eq. (11). After simple calculations, for the contribution to $\Omega(\omega,\mathbf{k})$ from this diagram, we obtain

$$\begin{aligned}\Omega^{(4)}(\omega,\mathbf{k}) = {} & \frac{E_{\mathbf{k}}}{\mathfrak{N}}\sum_{\mathbf{q}}\left[\frac{E_{\mathbf{q}}(1 + 2N_{\mathbf{q}}) - \epsilon_{\mathbf{q}}}{\epsilon_{\mathbf{q}}}\left(J_{\mathbf{k}} - J_0 + J_{\mathbf{q}} - J_{\mathbf{k}+\mathbf{q}} + \frac{1}{2}(Q_{\mathbf{q}}^{xx} + Q_{\mathbf{q}}^{yy} + Q_{\mathbf{k}}^{xx} + Q_{\mathbf{k}}^{yy} - 2Q_{\mathbf{k}+\mathbf{q}}^{zz} - 2Q_0^{xx})\right)\right. \\ & \left. - \frac{B_{\mathbf{q}}(1 + 2N_{\mathbf{q}})}{4\epsilon_{\mathbf{q}}}[Q_{\mathbf{k}}^{xx} - Q_{\mathbf{k}}^{yy} + 2(Q_{\mathbf{q}}^{xx} - Q_{\mathbf{q}}^{yy})]\right] \\ & - \frac{B_{\mathbf{k}}}{\mathfrak{N}}\sum_{\mathbf{q}}\left[\frac{E_{\mathbf{q}}(1 + 2N_{\mathbf{q}}) - \epsilon_{\mathbf{q}}}{2\epsilon_{\mathbf{q}}}\left(\frac{1}{2}(Q_{\mathbf{q}}^{xx} - Q_{\mathbf{q}}^{yy}) + Q_{\mathbf{k}}^{xx} - Q_{\mathbf{k}}^{yy}\right) - \frac{B_{\mathbf{q}}(1 + 2N_{\mathbf{q}})}{2\epsilon_{\mathbf{q}}}\left(J_{\mathbf{k}} + J_{\mathbf{q}} - 2J_{\mathbf{k}+\mathbf{q}} + \frac{1}{2}(Q_{\mathbf{q}}^{xx} + Q_{\mathbf{q}}^{yy} + Q_{\mathbf{k}}^{xx} + Q_{\mathbf{k}}^{yy} - 4Q_{\mathbf{k}+q}^{zz})\right)\right].\end{aligned} \tag{23}$$

At zero temperature, $N_{\mathbf{q}} = 0$ in Eq. (23). In this case, the spectrum is renormalized only by quantum fluctuations. As the temperature increases, corrections from terms in Eq. (23) containing $N_{\mathbf{q}}$ become larger. They exceed terms in Eq. (23) not containing $N_{\mathbf{q}}$ above a certain temperature. We find below that this temperature is of the order of $S\omega_0$. Then, it is convenient to separately discuss regimes $T \ll S\omega_0$ and $T \gg S\omega_0$.

#### 1. $T \ll S\omega_0$

By taking $N_{\mathbf{q}}=0$ in Eq. (23), in the leading order of $\omega_0$, we obtain

$$\Omega^{(4)}(\omega,\mathbf{k}) = Dk^2 \frac{S\omega_0\alpha}{2\mathfrak{N}} \sum_{\mathbf{q}} \frac{Q_{\mathbf{q}}^{xx} - Q_{\mathbf{q}}^{yy}}{\epsilon_{\mathbf{q}}} + \frac{S^2\omega_0\alpha}{8\mathfrak{N}} \sum_{\mathbf{q}} \frac{(Q_{\mathbf{q}}^{xx} - Q_{\mathbf{q}}^{yy})^2}{\epsilon_{\mathbf{q}}}. \tag{24}$$

Here, the first term is of the order of $k^2\omega_0^2 \ln(D/S\omega_0)$. Then it gives a negligibly small positive correction to the bare spectrum (14). In contrast, the second term in Eq. (24), being independent of $\mathbf{k}$, contributes to the spin-wave gap. It is much greater than the bare spectrum at $k \ll S\omega_0/D$.

#### 2. $T \gg S\omega_0$

Terms in Eq. (23) containing $N_{\mathbf{q}}$ come into play at such $T$ and, in the leading order of $\omega_0$, we have

$$\Omega^{(4)}(\omega,\mathbf{k}) = -(Dk^2)^2 \frac{2}{S} W(T) - Dk^2\omega_0\alpha[W(T)+V(T)] + \frac{S^2\omega_0\alpha}{8\mathfrak{N}} \sum_{\mathbf{q}} \frac{(Q_{\mathbf{q}}^{xx} - Q_{\mathbf{q}}^{yy})^2}{\epsilon_{\mathbf{q}}}, \tag{25}$$

$$W(T) = \frac{1}{\mathfrak{N}} \sum_{\mathbf{q}} \frac{J_0 - J_{\mathbf{q}}}{J_0} N_{\mathbf{q}} \approx w\left(\frac{T}{D}\right)^2, \tag{26}$$

$$V(T) = \frac{2}{\mathfrak{N}} \sum_{\mathbf{q}} N_{\mathbf{q}} \approx v \frac{T}{D} \ln\left(\frac{T}{S\omega_0}\right), \tag{27}$$

where $w=(16\pi)^{-1}\int_0^\infty dkk/(e^k-1)=\pi/96$ and $v=1/2\pi$. The first two terms in Eq. (25) do not change the structure of the bare spectrum, which results in the following renormalization of constants $D$ and $\omega_0$ in Eq. (14):

$$D \mapsto D\left[1 - \frac{1}{S}W(T)\right], \quad \omega_0 \mapsto \omega_0\left[1 - \frac{1}{S}V(T)\right]. \tag{28}$$

In contrast, the last term in Eq. (25) changes the form of the spectrum and contributes to the gap. Notice that the gap in Eq. (25) has the same form as in Eq. (24). Thermal corrections to the gap are small, which are of the order of $\omega_0^3 T \ln(T/S\omega_0)/D^2$.[27]

By comparing the first two terms in Eq. (25) with the first term in Eq. (24), one infers that thermal $k$-dependent corrections become much larger than quantum ones at $T \gg S\omega_0$.

### B. Loop diagram

We now turn to the loop diagram shown in Fig. 2(c). It originates from $\mathcal{H}_3$ terms (10) in the Hamiltonian. As a result of simple but tedious calculations, some details of which are presented in Appendix A, for the contribution to the real part of $\Omega(\omega,\mathbf{k})$ from this diagram at $k \ll 1$, we have

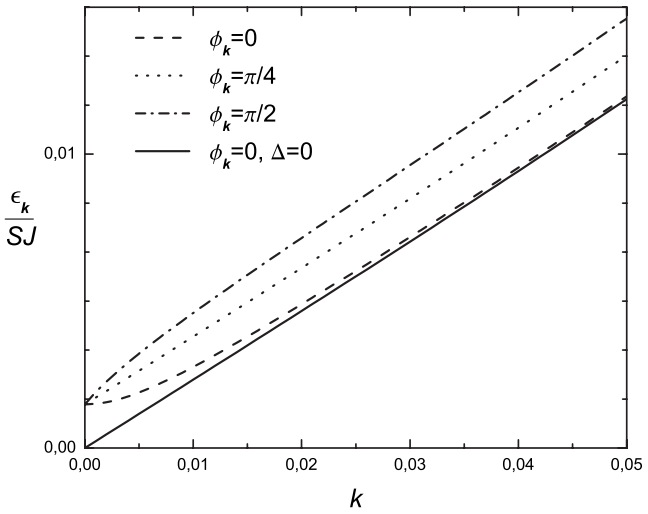


FIG. 3. Renormalized spin-wave spectrum at $\phi_{\mathbf{k}}=0$, $\phi_{\mathbf{k}}=\pi/4$, and $\phi_{\mathbf{k}}=\pi/2$ for a 2D FM at $T \ll S\omega_0$ with $\omega_0=0.05J$ and $S=1/2$. The bare spectrum at $\phi_{\mathbf{k}}=0$ (solid line) is also presented for comparison.

$$\mathrm{Re}\,\Omega^{(3)}(\omega,\mathbf{k}) = -\frac{S^2\omega_0\alpha}{2\mathfrak{N}} \sum_{\mathbf{q}} \frac{(Q_{\mathbf{q}}^{xz})^2}{\epsilon_{\mathbf{q}}}, \tag{29}$$

where we set $k=0$ under the sum because the summation over large $\mathbf{q}$ is essential. Notice that we discard in Eq. (29) all the terms that are much smaller than $\Omega^{(4)}(\omega,\mathbf{k})$, which are given by Eqs. (24) and (25). Temperature corrections to $\mathrm{Re}\,\Omega^{(3)}(\omega,\mathbf{k})$ are negligible.

### C. Resulting expressions

One can now derive the resulting expression for $\mathrm{Re}\,\Omega(\omega,\mathbf{k})$ by using Eqs. (24), (25), and (29).

#### 1. $T \ll S\omega_0$

From Eqs. (24) and (29), we obtain

$$\mathrm{Re}\,\Omega(\omega,\mathbf{k}) = Dk^2 \frac{S\omega_0\alpha}{2\mathfrak{N}} \sum_{\mathbf{q}} \frac{Q_{\mathbf{q}}^{xx} - Q_{\mathbf{q}}^{yy}}{\epsilon_{\mathbf{q}}} + \Delta^2, \tag{30}$$

$$\Delta = \sqrt{\alpha C S^2 \frac{\omega_0^3}{D}}, \tag{31}$$

where $C$ is given by Eq. (21). As mentioned above, $C \approx 0.0082$ for the simple square lattice with the exchange coupling only between nearest-neighbor spins. The first term in Eq. (30) originates from $\Omega^{(4)}(\omega,\mathbf{k})$, and both $\Omega^{(3)}(\omega,\mathbf{k})$ and $\Omega^{(4)}(\omega,\mathbf{k})$ contribute to the second term. The spin-wave gap $\Delta$ given by Eq. (31) is proportional to $\omega_0^{3/2}$. To illustrate this result, we plot in Fig. 3 the renormalized and bare spin-wave spectra for $\phi_{\mathbf{k}}=0$, $\phi_{\mathbf{k}}=\pi/4$, and $\phi_{\mathbf{k}}=\pi/2$, assuming that there is exchange coupling only between nearest-neighbor spins, $\omega_0=0.05J$, and $S=1/2$.

#### 2. $T \gg S\omega_0$

From Eqs. (25) and (29), one has

$$\mathrm{Re}\ \Omega(\omega,\mathbf{k}) = -(Dk^2)^2\frac{2}{S}W(T) - Dk^2\omega_0\alpha[W(T)+V(T)] + \Delta^2, \tag{32}$$

where $W(T)$, $V(T)$, and $\Delta$ are given by Eqs. (26), (27), and (31), respectively. Notice that the spin-wave gap $\Delta$ has the same form as that at $T \ll S\omega_0$ and thermal corrections to its square are negligible, which are of the order of $\omega_0^3 T^{3/2}/D^{5/2}$.

We infer from a comparison of Eq. (14) with Eqs. (30) and (32) that the renormalization of the bare spectrum is small at $T \ll D$ and $k \gg S\omega_0/D$. In contrast, the spectrum renormalization is significant at smaller $k$ due to the gap, which is much larger than all $k$-dependent terms at $k \lesssim (\Delta/S\omega_0)^2$. We use the renormalized spectrum below for a self-consistent calculation of the spin-wave damping and the estimation of higher order $1/S$ corrections.

## IV. SPIN-WAVE DAMPING

In this section, we discuss the imaginary part of $\Omega(\omega,\mathbf{k})$ to which only the loop diagram contributes shown in Fig. 2(c). Corresponding calculations are rather cumbersome and we discuss only the results here. One refers to Appendix A for some details of the calculations. We discuss 2D FMs on the simple square lattice in this section. Three regions should be considered: $k \gg \sqrt{S\omega_0/D}$, $S\omega_0/D \ll k \ll \sqrt{S\omega_0/D}$, and $k \lesssim (\Delta/S\omega_0)^2$ at which the real part of the spectrum has the form $\epsilon_\mathbf{k} \approx Dk^2$, $\epsilon_\mathbf{k} \approx k\sqrt{\alpha SD\omega_0}$, and $\epsilon_\mathbf{k} \approx \Delta$, respectively. $\mathrm{Im}\ \Omega(\omega,\mathbf{k})$ is an odd function of $\omega$ and we calculate it for $\omega = \epsilon_\mathbf{k}$ only. The spin-wave damping $\Gamma_\mathbf{k}$ at momentum $\mathbf{k}$ is found below by using the relation

$$\Gamma_\mathbf{k} = -\frac{\mathrm{Im}\ \Omega(\omega=\epsilon_\mathbf{k},\mathbf{k})}{2\epsilon_\mathbf{k}}. \tag{33}$$

### A. $k \gg \sqrt{S\omega_0/D}$

For $k \gg \sqrt{S\omega_0/D}$, one obtains

$$\Gamma_\mathbf{k} = \epsilon_\mathbf{k}\frac{S\omega_0^2}{D^2}\frac{1}{3\pi 2^8}\left[\left(1+24\frac{T}{S\omega_0 k}f(\phi_\mathbf{k})\right)\sin^2 2\phi_\mathbf{k} + \frac{3\pi-8}{4} + 6(\pi-2)\frac{T}{Dk^2}\right], \tag{34}$$

where

$$f(\phi_\mathbf{k}) = \int_0^\infty \frac{dq}{q^2 + q\cos^2\phi_\mathbf{k} + 4D\Delta^2/\alpha S^3\omega_0^3} \tag{35}$$

and $\Delta$ is given by Eq. (31). It is seen that the damping is anisotropic in this regime: it is smaller along the edges of the square and it reaches maxima along diagonals of the square.

### B. $S\omega_0/D \ll k \ll \sqrt{S\omega_0/D}$

For $S\omega_0/D \ll k \ll \sqrt{S\omega_0/D}$, one has

$$\Gamma_\mathbf{k} = \epsilon_\mathbf{k}\frac{S^2\omega_0^3}{D^3k^2}\frac{\alpha}{2^6\sqrt{3}\pi} \times\left[\left(\mathcal{A}_1(\mathbf{k}) + \frac{T}{\epsilon_\mathbf{k}}(\mathcal{A}_2(\mathbf{k})+\mathcal{A}_3(\mathbf{k}))\right)\sin^2 2\phi_\mathbf{k} + \frac{1}{20\alpha^3}\frac{D^3}{S^3\omega_0^3}k^6\left(\mathcal{B}_1(\mathbf{k}) - 3\mathcal{B}_2(\mathbf{k}) + \frac{9}{4}\mathcal{B}_3(\mathbf{k})\right) + \frac{T}{S\omega_0\alpha}\mathcal{B}_4\right], \tag{36}$$

where

$$\mathcal{A}_1(\mathbf{k}) = \int_{-\sqrt{1-\epsilon_1}}^{\sqrt{1-\epsilon_1}} \frac{dq}{\sqrt{\mathcal{L}(q,\mathbf{k})}}, \tag{37}$$

$$\mathcal{A}_2(\mathbf{k}) = 4\int_{-\sqrt{1-\epsilon_1}}^{\sqrt{1-\epsilon_1}} \frac{dq}{(1-q^2)\sqrt{\mathcal{L}(q,\mathbf{k})}}, \tag{38}$$

$$\mathcal{A}_3(\mathbf{k}) = 2\int_{\sqrt{1+\epsilon_2}}^{\infty} dq\frac{q+1}{q-1}\frac{1}{\sqrt{\mathcal{L}(q,\mathbf{k})}}, \tag{39}$$

$$\mathcal{B}_i(\mathbf{k}) = \frac{15}{4}\int_{-\sqrt{1-\epsilon_1}}^{\sqrt{1-\epsilon_1}} dq\frac{q^2}{(1-q^2)^{2i-2}}\mathcal{L}(q,\mathbf{k})^{(2i-1)/2}, \quad i=1,2,3, \tag{40}$$

$$\mathcal{B}_4 = 4\sqrt{3}\int_0^\infty dq\frac{(1+q^2)^{3/2}\sqrt{3+4q^2}}{(1+2q^2)^4} \approx 5.31, \tag{41}$$

$$\mathcal{L}(q,\mathbf{k}) = (1-q^2)^2 - \beta|1-q^2| - \xi(q^2+3), \tag{42}$$

$$\beta = \frac{2\alpha}{3}\frac{S^2\omega_0^2}{D^2k^3}\sin^2\phi_\mathbf{k}, \tag{43}$$

$$\xi = \frac{4}{3}\frac{\Delta^2}{D^2k^4}, \tag{44}$$

$$\varepsilon_1 = \tfrac{1}{2}[\beta - \xi + \sqrt{(\beta-\xi)^2+16\xi}], \tag{45}$$

$$\varepsilon_2 = \tfrac{1}{2}[\beta + \xi + \sqrt{(\beta+\xi)^2+16\xi}], \tag{46}$$

and $\mathcal{A}_{1,2}(\mathbf{k})$ and $\mathcal{B}_{1,2,3}(\mathbf{k})$ should be taken equal to zero at $\mathbf{k}$ such that $\varepsilon_1 \geq 1$, i.e., when the following inequality is satisfied:

$$1 - \beta - 3\xi \leq 0. \tag{47}$$

Notice that $\mathcal{L}(q,\mathbf{k})=0$ at $q = \pm\sqrt{1-\varepsilon_1}, \sqrt{1+\varepsilon_2}$ and it is positive inside the intervals $(-\sqrt{1-\varepsilon_1}, \sqrt{1-\varepsilon_1})$ and $(\sqrt{1+\varepsilon_2}, \infty)$. When $\beta, \xi \ll 1$, one has $\mathcal{A}_1(\mathbf{k}) \approx -\ln(\beta+\sqrt{\xi})$, $\mathcal{A}_{2,3}(\mathbf{k}) \sim 1/(\beta+\sqrt{\xi})$, and $\mathcal{B}_{1,2,3}(\mathbf{k}) \approx 1$. If $\beta, \xi \gtrsim 1$, we have $\mathcal{A}_3(\mathbf{k}) \sim 1/\sqrt{\beta+\xi}$. Terms in Eq. (36) containing $\mathcal{B}_i(\mathbf{k})$ and $\mathcal{B}_4$ play only at $|\sin 2\phi_\mathbf{k}| \ll 1$. In particular, from Eq. (36), we obtain that the spin-wave damping is zero at $T=0$ and $\mathbf{k}$ such that

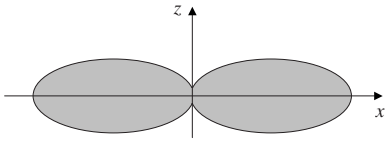


FIG. 4. The region in **k** plane is shown, in which the spin-wave damping is zero at $T=0$. This region is defined by Eq. (47). The linear dimension of the region is of the order of $(S\omega_0/D)^{2/3}$. The length of the region along the $z$ axis at $k_x=0$ is of the order of $(S\omega_0/D)^{3/4}$. As shown in Fig. 1, the $z$ axis is directed along the magnetization. The great thermal enhancement of the damping inside this region at $T \gg S\omega_0$ is illustrated by Figs. 5 and 6.

$\varepsilon_1 \geq 1$, i.e., when inequality (47) holds. The region determined by Eq. (47) is sketched in Fig. 4. From Eqs. (34) and (36), we conclude that the damping is small in the corresponding intervals provided that $\omega_0, T \ll D$.

### C. $k \ll S\omega_0/D$

As found above, the real part of the spectrum at $k \lesssim (\Delta/S\omega_0)^2$ is greatly renormalized, being approximately equal to $\Delta$. For $S\omega_0/D \gg k \gtrsim \Delta/\sqrt{TD}$, we self-consistently find

$$\Gamma_{\mathbf{k}} = \frac{\alpha}{2^8}\frac{T\omega_0^3 S^2}{D^2 \epsilon_{\mathbf{k}}}. \tag{48}$$

Notice that this regime is realized at a large enough temperature, $T \gg \omega_0$. At smaller $k$, $k \ll \Delta/\sqrt{TD} \ll S\omega_0/D$, or at small temperature, $T \ll \omega_0$, the spin-wave damping is exponentially small,

$$\Gamma_{\mathbf{k}} \propto \exp\left(-\frac{\Delta^2}{4TDk^2}\right). \tag{49}$$

It should be noted from Eqs. (36) and (48) that when $T \gg S\omega_0$, the damping $\Gamma_{\mathbf{k}}$ increases upon decreasing $k$ for $k \lesssim (S\omega_0/D)^{2/3}$. On the other hand, as we have just obtained, the damping is exponentially small at very small momenta $(k \ll \Delta/\sqrt{TD})$. Hence, one should observe a peak in $\Gamma_{\mathbf{k}}$ at $k \sim \Delta/\sqrt{TD}$ and at any **k** direction, the height of which can be estimated from Eq. (48). In particular, if the temperature is as large as the interval $(\Delta/S\omega_0)^2 \gg k \gtrsim \Delta/\sqrt{TD}$ is finite, i.e., if $T \gg S^2\omega_0/C$, we have $\epsilon_{\mathbf{k}} \approx \Delta$ at $k \sim \Delta/\sqrt{TD}$ in Eq. (48) and, for the peak height from Eq. (48) by using Eq. (31), one obtains

$$\frac{\Gamma_{\mathbf{k}}}{\epsilon_{\mathbf{k}}} = \frac{1}{2^8 C}\frac{T}{D}. \tag{50}$$

In a general case, the peak height cannot be larger than the value given by Eq. (50) because $\epsilon_{\mathbf{k}} \geq \Delta$ at $k \ll S\omega_0/D$. Notice also that Eq. (50) is valid for arbitrary $\phi_{\mathbf{k}}$.

It is seen from Eq. (50) that the spin-wave damping is much smaller than the real part of the spectrum if $T \ll D, T_C$, where

$$T_C = \frac{4\pi DS}{\ln\{4\pi S[D/(S\omega_0)]^{3/2}\}} \tag{51}$$

is the value of the Curie temperature for $S \sim 1$ obtained by using the spin-wave theory (see Sec. VI).[28] On the other hand, the temperature can be greater than $D$ for large spin values much greater than unity, $S \gtrsim \ln\{4\pi S[D/(S\omega_0)]^{3/2}\}$,[29] so that $D < T \ll T_C^{(S\gg 1)}$, where

$$T_C^{(S\gg 1)} = \frac{8\pi DS}{3\ln[D/(S\omega_0)]} \tag{52}$$

is the Curie temperature in the spin-wave approximation for $S \gg \ln\{4\pi S[D/(S\omega_0)]^{3/2}\}$. Then one might conclude from Eq. (50) that the damping can be much larger than the real part of the spectrum. In the meantime, we show in Sec. V that the temperature correction to the spin-wave gap is large at such large $T$ and $S$. As a result, the imaginary part of the spectrum is also much smaller than the real part at $S \gg 1$ and $D < T \ll T_C^{(S\gg 1)}$ and the peak height of the ratio $\Gamma_{\mathbf{k}}/\epsilon_{\mathbf{k}}$ in quantum 2D FM cannot be larger than that in the classical 2D FM, which is approximately equal to 0.16 for the simple square lattice with exchange coupling only between nearest spins.

We sketch the dependence of $\Gamma_{\mathbf{k}}$ on the momentum in Fig. 5 at $k \ll 1$, $S \sim 1$, and $T \gg S\omega_0$ by taking into account the results obtained in this section. It is seen that the damping is highly anisotropic at $k \gtrsim S\omega_0/D$. The damping increases with decreasing $k$ up to $k \sim \Delta/\sqrt{TD}$ if **k** is directed along a square edge (i.e., if $|\sin 2\phi_{\mathbf{k}}| = 0$). In contrast, the damping is not a monotonic function of $k$ for $|\sin 2\phi_{\mathbf{k}}| \sim 1$: it decreases with decreasing $k$ up to $k \sim (S\omega_0/D)^{2/3}$ and then it rises up to $k \sim \Delta/\sqrt{TD}$. The damping is only slightly anisotropic in the interval $\Delta/\sqrt{TD} \lesssim k \lesssim S\omega_0/D$. A peak exists at $k \sim \Delta/\sqrt{TD}$ at any given $\phi_{\mathbf{k}}$, the height of which can be estimated by using Eq. (48). This peak is followed by an exponential decay of the damping at $k < \Delta/\sqrt{TD}$ having the form (49).

To illustrate in more detail the region of small momenta $k \ll \sqrt{S\omega_0/D}$ in which the peak exists, we derive general expressions for $\Gamma_{\mathbf{k}}$ which coincide with Eq. (36) at $k \gg S\omega_0/D$ and with Eqs. (48) and (50) at $\Delta/\sqrt{TD} \lesssim k \ll S\omega_0/D$. These general expressions appear to be quite cumbersome for arbitrary $\phi_{\mathbf{k}}$. Then, we present here only the equation in the special case of $\sin \phi_{\mathbf{k}} = 0$, which is the simplest one:

$$\frac{\Gamma_{\mathbf{k}}}{\epsilon_{\mathbf{k}}} = \frac{\alpha^2 S^3 \omega_0^4}{16\pi D^2 \Delta^2}\frac{1}{t}\frac{\sqrt{1+\kappa^2}}{\kappa^3}\int_{\zeta}^{\infty} dq \frac{\exp(q\sqrt{1+q^2}/t)}{[\exp(q\sqrt{1+q^2}/t)-1]^2} \times \frac{q(1+q^2)^{5/2}}{(1+2q^2)^3}\sqrt{1-\frac{1+q^2}{(1+2q^2)^2}\frac{1+\kappa^2}{\kappa^2}}, \tag{53}$$

where $\kappa = k\sqrt{SD\omega_0\alpha}/\Delta$, $t = T/(S\omega_0\alpha)$, and

$$\zeta = \sqrt{\frac{1}{8\kappa^2}(1 - 3\kappa^2 + \sqrt{9\kappa^4 + 10\kappa^2 + 1})}. \tag{54}$$

At $q = \zeta$, the expression under the square root in Eq. (53) is equal to zero and it is positive for $q > \zeta$. When $1 \gg \kappa \gtrsim \sqrt{S\omega_0\alpha/T}$ (i.e., when $\Delta/\sqrt{SD\omega_0} \gg k \gtrsim \Delta/\sqrt{TD}$) and $T \gg S\omega_0$, Eq. (53) transforms into Eq. (48). In the opposite limiting case of $\kappa \gg 1$ (to be precise, at $\Delta/\sqrt{SD\omega_0} \ll k$

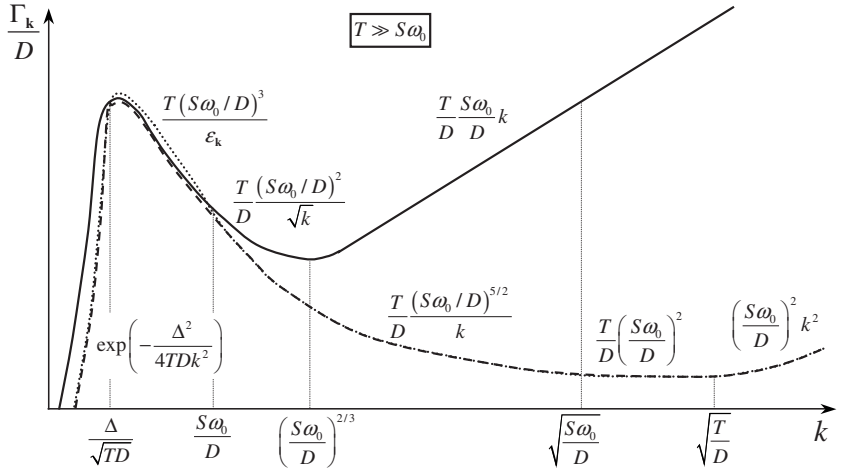


FIG. 5. Sketch of the spin-wave damping $\Gamma_{\mathbf{k}}$ versus the momentum at $k \ll 1$ for $|\sin 2\phi_{\mathbf{k}}| \sim 1$ (solid line), $|\sin \phi_{\mathbf{k}}| = 1$ (dashed line), and $|\sin \phi_{\mathbf{k}}| = 0$ (dotted line). The corresponding dependences of $\Gamma_{\mathbf{k}}$ on $T$, $\omega_0$, and $k$ are also indicated. We imply $S \sim 1$ and $T \gg S\omega_0$. Curves for $|\sin \phi_{\mathbf{k}}| = 1$ and $|\sin \phi_{\mathbf{k}}| = 0$ differ only slightly in the interval $\Delta/\sqrt{TD} \lesssim k \ll S\omega_0/D$. Notice that the ratio $\Gamma_{\mathbf{k}}/\epsilon_{\mathbf{k}}$ rises with decreasing $k$ for any given $\phi_{\mathbf{k}}$ at $k \gtrsim \Delta/\sqrt{TD}$ and there exist a peak at $k \sim \Delta/\sqrt{TD}$ and an exponential decay at $k \lesssim \Delta/\sqrt{TD}$. The ratio $\Gamma_{\mathbf{k}}/\epsilon_{\mathbf{k}}$ is shown in the vicinity of the peak in Fig. 6.

$\ll \sqrt{S\omega_0/D}$), one obtains the last term in Eq. (36) from Eq. (53) at $T \gg S\omega_0$.

We plot in Fig. 6 the ratio of the spin-wave damping and the real part of the spectrum given by Eq. (53) versus the reduced wave vector $\kappa$ for 2D FMs with $S=1/2$ and $S=3$ on the simple square lattice assuming that $\omega_0=0.01J$. The peak is seen at $\kappa \sim \sqrt{S\omega_0\alpha/T}$ (i.e., at $k \sim \Delta/\sqrt{TD}$). Its position moves to a smaller $\kappa$ and the height rises as $S$ increases at a given ratio $T/T_C$ or as $T$ increases at a given $S$.

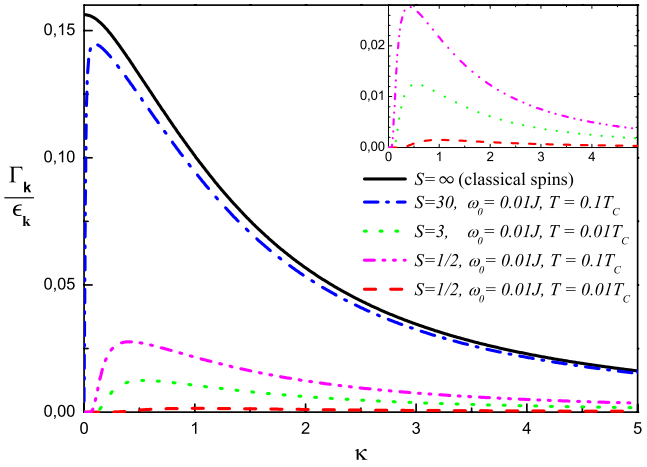


FIG. 6. (Color online) The ratio of the spin-wave damping and the real part of the spectrum $\Gamma_{\mathbf{k}}/\epsilon_{\mathbf{k}}$ versus the reduced wave vector $\kappa$ at $\sin \phi_{\mathbf{k}}=0$ for the classical and quantum 2D FMs on the simple square lattice. The ratios $\Gamma_{\mathbf{k}}/\epsilon_{\mathbf{k}}$ are given by Eqs. (63) and (53), wherein $\kappa=k\sqrt{j^3/(C_{\gg}w^2T)}$ and $\kappa=k\sqrt{SD\omega_0\alpha/\Delta_{\gg}}$ for the classical and quantum FMs, respectively, wherein $\Delta_{\gg}$ is given by Eq. (55). The curve for classical spins is for $T \ll j$ and $w \ll j$ [see Eq. (61)]. There are peaks at $\kappa \sim \sqrt{S\omega_0\alpha/T}$ in quantum 2D FMs. Inset: The same is shown for $S=1/2$ and $S=3$ on a large scale. For all quantum magnets, the boundary of the area shown in Fig. 4, wherein the spin-wave damping is zero at $T=0$, is located at $\kappa \gtrsim 10$.

## V. LARGE SPINS

Let us now consider large spins $S \gtrsim \ln\{4\pi S[D/(S\omega_0)]^{3/2}\}$. As explained in Sec. IV, the temperature can be of the order of $D$ in this case, remaining much smaller than the Curie temperature. When $T \sim D$, one can use expressions for $\Omega(\omega,\mathbf{k})$ obtained above with the exception for the gap: the temperature correction becomes important and, for the gap in Eq. (32), one has

$$\Delta_{\gg}^2 = \Delta^2 + \frac{S\omega_0\alpha}{\mathfrak{N}}\sum_{\mathbf{q}}\frac{(E_{\mathbf{q}}-B_{\mathbf{q}})N_{\mathbf{q}}}{\epsilon_{\mathbf{q}}}\left[(Q_{\mathbf{q}}^{xx}-Q_{\mathbf{q}}^{zz}) - \frac{S(E_{\mathbf{q}}-B_{\mathbf{q}})(Q_{\mathbf{q}}^{xz})^2}{\epsilon_{\mathbf{q}}^2}\left(1+\frac{\epsilon_{\mathbf{q}}}{T}(1+N_{\mathbf{q}})\right)\right], \quad (55)$$

where $\Delta$ is given by Eq. (31), the first and second terms in the square brackets stem from the Hartree–Fock and the loop diagrams shown in Figs. 2(b) and 2(c), respectively.

Let us discuss temperatures $2SJ_0 < T \ll T_C^{(S\gg 1)}$, where $2SJ_0$ is the spin-wave bandwidth and $T_C^{(S\gg 1)}$ is given by Eq. (52). To find corrections to the spectrum at such a large $T$, one can expand all the Planck functions under sums over momenta up to the first term: $N_{\mathbf{q}} \approx T/\epsilon_{\mathbf{q}}$. Then, we have Eq. (32) for the real part of $\Omega(\omega,\mathbf{k})$, where

$$W(T) = \frac{T}{SJ_0}, \quad V(T) = \frac{T}{2\pi D}\ln\left(\frac{D}{S\omega_0}\right) \quad (56)$$

now and, for the gap from Eq. (55), one obtains

$$\Delta_{\gg} = \sqrt{\Delta^2 + \alpha C_{\gg} S^2 \frac{\omega_0^3}{D^2}T}, \quad (57)$$

$$C_{\gg} = \frac{D^2}{\omega_0^2 \mathfrak{N}} \sum_{\mathbf{q}} \frac{(Q_{\mathbf{q}}^{xx} - Q_{\mathbf{q}}^{zz})^2 - 4(Q_{\mathbf{q}}^{xz})^2}{2\epsilon_{\mathbf{q}}^2}, \tag{58}$$

where we can discard $\Delta^2$ under the square root in Eq. (57) because of its smallness as compared to the second term at $T \gg D$. The summation over large momenta gives the main contribution in Eq. (58) and, as a result of a numerical computation for the coupling only between nearest-neighbor spins on the simple square lattice, we find $C_{\gg} \approx 0.025$.

A wide region appears in the momentum space in which the bare spectrum is much larger than the gap and has the form $\epsilon_{\mathbf{k}}^2 \approx S\omega_0 \alpha [Dk^2 + (S\omega_0 k/2)\sin^2 \phi_{\mathbf{k}}]$. The corresponding interval in $\mathbf{k}$ space is given by $(\Delta_{\gg}/S\omega_0)^2 \lesssim k \ll S\omega_0/D$ for $|\sin \phi_{\mathbf{k}}| \sim 1$ and by $\Delta_{\gg}/\sqrt{SD\omega_0} \ll k \ll S\omega_0/D$ for $|\sin \phi_{\mathbf{k}}| \ll 1$. As a result, all of the expressions for the damping obtained above should be reconsidered. In particular, Eq. (34) is valid only for $k \gg S\sqrt{\omega_0/T}$. All $T$-independent terms are negligible in Eq. (34) and one should use expression (57) for the gap rather than Eq. (31). Then, Eqs. (34) and (36) are not valid at $\sqrt{S\omega_0/D} \ll k \ll S\sqrt{\omega_0/T}$ and $S\omega_0/D \ll k \ll \sqrt{S\omega_0/D}$, respectively, because an integration over the above mentioned interval in the momentum space is essential in the corresponding sums. The results are quite cumbersome and we do not present them here. The main conclusion is that the spin-wave damping is much smaller than the real part of the spectrum at $k \gg S\omega_0/D$. Let us discuss in some detail only the damping at small momenta $k \ll S\omega_0/D$ because the diffusion mode was proposed in Refs. 9 and 10 at small $k$.

The ratio of the spin-wave damping and the real part of the spectrum at $(\Delta_{\gg}/S\omega_0)^2 \gg k \gtrsim \Delta_{\gg}/\sqrt{TD}$ can be found from Eq. (50) (replacing $\Delta$ with $\Delta_{\gg}$) with the result

$$\frac{\Gamma_{\mathbf{k}}}{\Delta_{\gg}} = \frac{1}{2^8 C_{\gg}}. \tag{59}$$

This expression gives the approximate value of the peak height on the curve $\Gamma_{\mathbf{k}}/\epsilon_{\mathbf{k}}$ that is valid for all $\phi_{\mathbf{k}}$. The right part of Eq. (59) is approximately equal to 0.16 for the exchange coupling only between nearest-neighbor spins on the simple square lattice. It is interesting to note that the smallness of the spin-wave damping in this case is *numerical,* whereas at $S \sim 1$, the smallness is parametric [see Eq. (50)]. Notice that at $k \ll \Delta_{\gg}/\sqrt{TD}$, the damping is exponentially small, as discussed in Sec. IV C.

It is seen from Eq. (59) that the value of the peak height is inversely proportional to $C_{\gg}$, which depends on the exchange coupling between spins $J_{lm}$ [see Eq. (58)]. It is interesting to examine the dependence of $\Gamma_{\mathbf{k}}/\Delta_{\gg}$ as given by Eq. (59) on the value of the coupling between next-nearest neighbors which, in particular, can significantly reduce $D$. We assume that the exchange coupling between nearest- and next-nearest-neighbor spins are equal to $J$ and $J'$, respectively (see the inset in Fig. 7). For the spin-wave stiffness in this case, one has $D = SJ(1+2J'/J)$. The dependence of the peak height on $D/SJ$ is shown in Fig. 7. It is seen that even at very small $D$, i.e., for frustrating next-nearest-neighbor interaction, magnons are well-defined quasiparticles. Importantly, it is implied even in the case of small $D$ that $D$

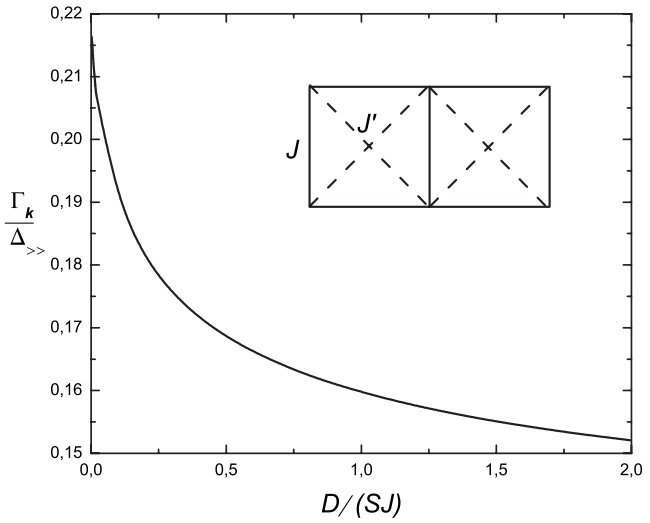


FIG. 7. The peak height on the curve for $\Gamma_{\mathbf{k}}/\epsilon_{\mathbf{k}}$ given by Eq. (59) versus the dimensionless spin-wave stiffness $D/(SJ)$ for 2D FM with $S \gg 1$ and with the next-nearest-neighbor exchange coupling $J'$ (see the inset). One has $D = SJ(1+2J'/J)$ in this case and it is implied that $D \gg S\omega_0$ and $8S(J+J') \ll T \ll T_C \propto SD$ even for small $D$, wherein $8S(J+J')$ is the spin-wave bandwidth.

$\gg S\omega_0$ and $8S(J+J') \ll T \ll T_C^{(S \gg 1)} \propto SD$, where $8S(J+J')$ is the spin-wave bandwidth.

We do not present here expressions for the damping at $(\Delta_{\gg}/S\omega_0)^2 \lesssim k \lesssim S\omega_0/D$ for arbitrary $\phi_{\mathbf{k}}$. The main conclusion is that the damping is much smaller than the real part of the spectrum. To illustrate this, let us consider only $\sin \phi_{\mathbf{k}} = 0$. The bare spectrum has the minimum value at $\sin \phi_{\mathbf{k}} = 0$ for a given $k$ in the discussed momentum interval and it is the most "dangerous" case, in which one could expect a large spin-wave damping as compared with the real part of the spectrum. Corresponding calculations give Eq. (53) for the damping at $k \ll \sqrt{S\omega_0/D}$, where one should replace $\Delta$ with $\Delta_{\gg}$. We use this modification of Eq. (53) to plot $\Gamma_{\mathbf{k}}/\epsilon_{\mathbf{k}}$ in Fig. 6 for $S = 30$, $\omega_0 = 0.01J$, and $T = 0.1T_C^{(S \gg 1)}$.

### Classical spins

To find the spectrum renormalization in the classical 2D FMs by using the spin-wave formalism discussed in the present paper, one should consider the limit of

$$S \to \infty, \quad \hbar \to 0, \quad J, \omega_0 \to 0 \tag{60}$$

assuming that

$$\hbar S = \text{const}, \quad JS^2 = j = \text{const}, \quad \omega_0 S^2 = w = \text{const}, \tag{61}$$

and $T/j$ is much smaller than unity. Moreover, one should replace operators of creation and annihilation $a_{\mathbf{k}}, a_{\mathbf{k}}^{\dagger}$ with classical operators $\beta_{\mathbf{k}} = a_{\mathbf{k}}/\sqrt{S}$, $\beta_{\mathbf{k}}^{\dagger} = a_{\mathbf{k}}^{\dagger}/\sqrt{S}$, the Bose occupation numbers of which are finite.[30,31] As a result, the spectrum and corrections to it in the classical limit can be obtained from the expressions found above by multiplying them by $S$ and taking the limit (60) with the assumptions (61). In particular, for the gap in the classical 2D FM from Eq. (57), we have

$$\Delta_\infty = \sqrt{\alpha C_\gg \frac{w^3}{j^2} T}. \tag{62}$$

Only the second term under the square root in Eq. (57) contributes to $\Delta_\infty^2$. Notice that there is no exponential decay of the damping at small $k$ in classical 2D FM in which Eq. (59) is valid at all $k$ much smaller than $C_\gg wT/j^2$ because $\Delta_\gg/\sqrt{TD} \to 0$ when $S \to \infty$. Then, the peaks in $\Gamma_\mathbf{k}$ and $\Gamma_\mathbf{k}/\epsilon_\mathbf{k}$ are located at $k=0$.

In particular, one obtains the following in the limiting case of classical spins from Eq. (53) by expanding the exponents in $t$ and replacing $\Delta$ with $\Delta_\infty$:

$$\frac{\Gamma_\mathbf{k}}{\epsilon_\mathbf{k}} = \frac{1}{16\pi C_\gg} \frac{\sqrt{1+\kappa^2}}{\kappa^3} \int_\zeta^\infty dq \frac{(1+q^2)^{3/2}}{q(1+2q^2)^3} \times \sqrt{1 - \frac{1+q^2}{(1+2q^2)^2} \frac{1+\kappa^2}{\kappa^2}}, \tag{63}$$

where $\kappa = k\sqrt{j^3/C_\gg w^2 T}$ now and $\zeta$ is given by Eq. (54). Equation (63) transforms into Eq. (59) at $\kappa \ll 1$ (with $\Delta_\infty$ put instead of $\Delta_\gg$). We also plot in Fig. 6 the ratio of the spin-wave damping and the real part of the spectrum given by Eq. (63) versus the reduced wave vector $\kappa$ for the classical 2D FM on the simple square lattice. As pointed out above, the position of the peak on quantum curves moves to smaller $\kappa$ and the peak height rises as $S$ increases at a given ratio $T/T_C$ or as $T$ increases at a given $S$. However, as demonstrated above and as seen by the example of $S=1/2$, $S=3$, and $S=30$ shown in Fig. 6, the peaks on the quantum curves cannot be higher than that of the classical 2D FM located at $k=0$, the height of which is given by Eq. (59). It should be noted here that the peak height for finite $S \gg 1$ and $D \ll T \ll T_C^{(S\gg 1)}$ is slightly smaller than that given by Eq. (59) because we have discarded $\Delta^2$ under the square root in Eq. (57) by deriving Eq. (59). On the other hand, Eq. (59) gives the precise value of the peak height for a classical 2D FM because $\Delta^2$ disappears after taking the limit (60) with the assumptions (61) and only the second term under the square root in Eq. (57) contributes to the gap.

## VI. DISCUSSION

In this section, we address five questions: (i) the relation between the anisotropic term (20) in the total energy of a 2D FM and the spin-wave gap (31), (ii) the discussion of the further order $1/S$ corrections, (iii) the calculation of the magnetization taking into account the spin-wave spectrum renormalization, (iv) the derivation of the spin Green's functions in the first order of $1/S$, and (v) the brief discussion of the effect of the easy-plane anisotropy and the spectrum renormalization obtained in Refs. 9 and 10.

(i) As discussed in Sec. I, it looks reasonable that the dipolar in-plane anisotropy given by Eq. (20) should be accompanied with a spin-wave gap. The relation between this anisotropy and the gap can be shown for a 2D FM in the same nonrigorous manner as for a 3D FM.[11] Let us discuss large spins and try to take into account the dipolar in-plane anisotropy (20) phenomenologically by adding to the microscopic Hamiltonian (2) the following expression [cf. Eq. (20)]:

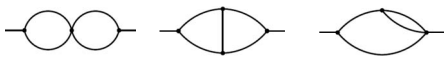

FIG. 8. Some diagrams of the second order in $1/S$.

$$C\frac{\omega_0^2}{2S^2 D} \sum_l (S_l^x)^2 (S_l^z)^2. \tag{64}$$

After Dyson–Maleev transformation (8), this term gives the contribution $CS\omega_0^2/(4D)(a_\mathbf{k}^\dagger + a_\mathbf{k})^2$ to the bilinear part (9) of the Hamiltonian that, in turn, leads to the shift $E_\mathbf{k} \mapsto E_\mathbf{k} + CS\omega_0^2/2D$ and $B_\mathbf{k} \mapsto B_\mathbf{k} + CS\omega_0^2/2D$. By using this renormalization of $E_\mathbf{k}$ and $B_\mathbf{k}$ and Eq. (14) for the spectrum, one recovers the spin-wave gap (31) in Eq. (30). This consideration does not work for $S=1/2$ because Eq. (64) is a constant in this case.

(ii) Let us turn to further order $1/S$ corrections. Some diagrams of the second order in $1/S$ are presented in Fig. 8. It can be shown that at least their real parts are much smaller than the real parts of the first order diagrams discussed above. To demonstrate this, one has to take into account the fact that the spin-wave gap screens infrared singularities appearing in some of these diagrams. Moreover, three- and four-particle vertices contain additional smallness at small external momenta. Thus, the three-particle vertex (10) contains the $xz$ component of the dipolar tensor, which is proportional to the product of $\omega_0$ and momentum [see Eq. (5)]. As for a four-particle vertex, the expression under the sum in Eq. (11) at $k_{1,2,3,4} \ll 1$ has the form

$$2\mathbf{k}_3(2\mathbf{k}_1 + \mathbf{k}_3) a_{-1}^\dagger a_{-2}^\dagger a_3 a_4 - \omega_0 k_2 \frac{1+\sin^2 \phi_{\mathbf{k}_2}}{2} a_{-1}^\dagger a_2 a_3 a_4 + \frac{\omega_0}{2}(k_2 \sin^2 \phi_{\mathbf{k}_2} + 2|\mathbf{k}_2 + \mathbf{k}_3| \cos^2 \phi_{\mathbf{k}_2+\mathbf{k}_3}) a_{-1}^\dagger a_{-2}^\dagger a_3 a_4 + \alpha\omega_0 a_{-1}^\dagger (a_2 - a_{-2}^\dagger) a_3 a_4. \tag{65}$$

It is seen that the first term in Eq. (65) is quadratic in momenta. The second and third ones are proportional to $\omega_0$ and momenta. The last term in Eq. (65) is proportional only to $\omega_0$, but the combination $a_2 - a_{-2}^\dagger$ involved in it is "soft": for instance, its coupling with operator $a_{-2}$ gives $F(\omega_2, \mathbf{k}_2) - \bar{G}(\omega_2, \mathbf{k}_2) \approx -(Dk_2^2 + S\omega_0 k_2 \sin^2 \phi_{\mathbf{k}_2}/2 - \omega_2)/\mathcal{D}(\omega_2, \mathbf{k}_2)$, which is much smaller than $F(\omega_2, \mathbf{k}_2)$ or $\bar{G}(\omega_2, \mathbf{k}_2)$ themselves [$F(\omega_2, \mathbf{k}_2) \approx G(\omega_2, \mathbf{k}_2) \sim S\omega_0/\mathcal{D}(\omega_2, \mathbf{k}_2)$ at $k_2 \ll \sqrt{S\omega_0/D}$ and $\omega_2 \ll S\omega_0$]. As a result, further order diagrams appear to be small at $T \ll T_C$.

Unfortunately, the smallness of the three- and four-particle vertices was not taken into account in my previous paper,[11] which was devoted to 3D FMs in a similar qualitative discussion of further order $1/S$ corrections. As a result, further order corrections were overestimated there. It was proposed that they are small only at $T \ll \omega_0$, whereas the range of the validity of the perturbation theory is much wider in 3D FMs: $T \ll T_C$.

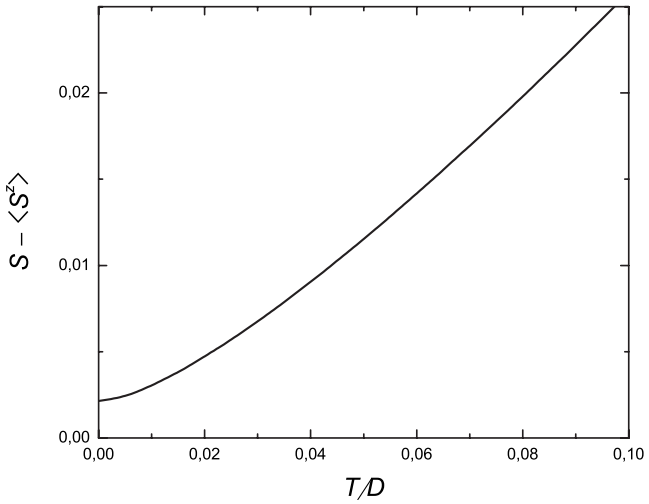


FIG. 9. The value $S-\langle S^z\rangle$ given by Eq. (66) versus the dimensionless temperature $T/D$ for the square 2D FM with $\omega_0=0.1J$.

(iii) Let us calculate now the magnetization value $\langle S^z\rangle$ by using a renormalized spectrum. After a simple computation, we have

$$\frac{S-\langle S^z\rangle}{S}=\frac{1}{\mathfrak{N}}\sum_{\mathbf{q}}\frac{E_{\mathbf{q}}(1+2N_{\mathbf{q}})-\epsilon_{\mathbf{q}}}{2S\epsilon_{\mathbf{q}}}=\begin{cases}\dfrac{T}{4\pi DS}\ln\left[\dfrac{T}{D}\left(\dfrac{D}{S\omega_0}\right)^{3/2}\right], & T\gg\dfrac{S\omega_0}{\ln(D/[S\omega_0])}\\ \dfrac{\omega_0\alpha}{16\pi D}, & T\ll\dfrac{S\omega_0}{\ln(D/[S\omega_0])}.\end{cases}\tag{66}$$

Notice that zero-point fluctuations give the main contribution at $T\ll S\omega_0/\ln[D/(S\omega_0)]$. The value $S-\langle S^z\rangle$ given by Eq. (66) is shown in Fig. 9 for $\omega_0=0.1J$. It should be pointed out also that taking into consideration the gap in the spectrum does not change the form of the magnetization. In the meantime, Eq. (66) differs from the corresponding expression in Ref. 4. The origin of this discrepancy is discussed in Appendix B. The value of the Curie temperature (51) given by the spin-wave theory follows from Eq. (66) by setting $\langle S^z\rangle$ to be equal to zero. In the case of large spins $S\gtrsim\ln\{4\pi S[D/(S\omega_0)]^{3/2}\}$, Planck's function in Eq. (66) can be expanded and one finds Eq. (52) for the Curie temperature by setting $\langle S^z\rangle=0$.

(iv) Spin Green's functions defined as $\chi_{ij}(\omega,\mathbf{k})=i\int_0^\infty dt e^{i\omega t}\langle[S^i_{-\mathbf{k}}(t),S^j_{\mathbf{k}}(0)]\rangle$ can be straightforwardly calculated in the first order of $1/S$ by using Eqs. (16)–(18) and expressions for the self-energy parts with the following results for the transverse components:

$$\chi_{xx}(\omega,\mathbf{k})=-S\frac{Dk^2+S\omega_0\alpha}{\omega^2-\epsilon_{\mathbf{k}}^2-\Omega(\omega,\mathbf{k})},\tag{67}$$

$$\chi_{yy}(\omega,\mathbf{k})=-S\frac{Dk^2+(S\omega_0/2)k\sin^2\phi_{\mathbf{k}}+\Delta^2/(S\omega_0\alpha)}{\omega^2-\epsilon_{\mathbf{k}}^2-\Omega(\omega,\mathbf{k})},\tag{68}$$

where $\epsilon_{\mathbf{k}}$ is the bare spectrum here. Corrections from the self-energy parts to the numerator are negligible in Eq. (67). In contrast, the numerator in Eq. (68) for $\chi_{yy}(\omega,\mathbf{k})$ greatly renormalizes at small $k$ so that the uniform susceptibility $\chi_{yy}(\omega,\mathbf{0})$ becomes finite.

The corresponding expression for the longitudinal component $\chi_{zz}(\omega,\mathbf{k})$ is slightly more cumbersome. It can be calculated by using Eqs. (A2a)–(A2c). Let us discuss only uniform longitudinal susceptibility $\chi_{zz}(\omega,\mathbf{0})$. For $|\omega|\gg\sqrt{(S\omega_0)^3/D}\gg\Delta$, we have

$$\chi_{zz}(\omega,\mathbf{0})=\frac{TS\omega_0\alpha}{4D}\frac{1}{\omega^2}\left(\frac{2}{\pi}\ln\left|\frac{2\Delta}{\omega}\right|+i\,\mathrm{sgn}(\omega)\right).\tag{69}$$

For the imaginary part, when $|\omega|\lesssim\sqrt{(S\omega_0)^3/D}$, one obtains

$$\mathrm{Im}\,\chi_{zz}(\omega,\mathbf{0})=\mathrm{sgn}(\omega)\theta(|\omega|-2\Delta)\frac{\alpha^{3/4}\Gamma(3/4)^2}{\sqrt{2\pi^3}}\frac{T(S\omega_0)^{1/4}}{D^{3/4}}\frac{(\omega^2-4\Delta^2)^{1/4}}{\omega^2},\tag{70}$$

where $\Gamma(x)$ is the gamma function and $\theta(x)$ is the Heaviside step function [$\theta(x)=1$ when $x>0$ and $\theta(x)=0$ when $x<0$]. The corresponding expression for the real part of $\chi_{zz}(\omega,\mathbf{0})$ is quite cumbersome and we do not present it here. It is seen from Eq. (70) that $\mathrm{Im}\,\chi_{zz}(\omega,\mathbf{0})=0$ at $\omega<2\Delta$. In contrast, if one did not take into account the spin-wave gap $\Delta$, the infrared singularity would appear in the form of $\mathrm{Im}\,\chi_{zz}(\omega\to0,\mathbf{0})\sim\omega^{-3/2}$. Such a singularity is a nonphysical one since it leads to an infinitely large absorption function[32] $Q_\omega\propto\omega\,\mathrm{Im}\,\chi(\omega)$ at $\omega=0$. A similar situation exists in 3D FMs with dipolar forces. The infrared singularity in the form of $\mathrm{Im}\,\chi_{zz}(\omega\to0,\mathbf{0})\sim T/\omega$ can be found by not taking into account the spin-wave gap.[6] This singularity leads to the finite absorption function at $\omega=0$, which signifies that the sample would be heated by a dc field. On the other hand, the spin-wave gap screens this singularity, which leads to zeroth $Q_\omega$ at $\omega=0$.[11]

(v) We will discuss the effect of the exchange anisotropy that has the form

$$\mathcal{H}_a=\frac{1}{2}\sum_{l\neq m}A_{lm}S_l^yS_m^y.\tag{71}$$

and the one-ion anisotropy $\Sigma_l A(S_l^y)^2$ in detail elsewhere. The corresponding renormalization of the above results for the real part of the spectrum is discussed briefly in Appendix C by taking into account the exchange anisotropy (71). In particular, it is shown there that expressions (31) and (57) for the gap should be multiplied by the factor $\sqrt{\tilde{\omega}_0/\omega_0}$, where

$$\tilde{\omega}_0=\omega_0+\frac{A_0}{\alpha}.\tag{72}$$

In the limiting case of classical spins, in addition to Eqs. (60) and (61), one should imply that $A\to0$ and $AS^2=\mathrm{const}$. Then,

we will assume that $\tilde{\omega}_0 S^2=\tilde{w}=$const and, for the gap in classical 2D FMs, one has Eq. (62) multiplied by $\sqrt{\tilde{w}/w}$.

The classical 2D FM with dipolar interaction and easy-plane anisotropy was discussed in Refs. 9 and 10. The existence of the easy-plane anisotropy seems not to be crucial for the results obtained in Refs. 9 and 10. The condition $\sqrt{\tilde{w}/j} \gg w/j$, which is important for the consideration in these papers, holds also at $A=0$ ($\tilde{w}=w$) if $w \ll j$, which is also implied there. The spin-wave gap (62) (multiplied by $\sqrt{\tilde{w}/w}$) was not taken into account in Refs. 9 and 10. A great renormalization of the spin-wave spectrum at small enough momenta was obtained there. In particular, a diffusion mode (DM) was found at $k \ll k_{\mathrm{DM}} \sim wt^{3/4}/[j \ln^{1/4}(\sqrt{j\tilde{w}/w})]$, where $t=T/4\pi j$. In the meantime, the spin-wave gap screens all of the spectrum peculiarities obtained in Refs. 9 and 10. For example, at $|\sin \phi_{\mathbf{k}}| \ll 1$, the energy of the diffusion mode has the form that is up to a numerical factor of the order of unity $-ik^2t^{-1/4} \ln^{5/4}(\sqrt{j\tilde{w}/w})\sqrt{\tilde{w}j^3/w^2}$. The spin-wave gap given by Eq. (62) multiplied by $\sqrt{\tilde{w}/w}$ is much larger than the energy of the diffusion mode at $k \ll k_{\mathrm{DM}}$.

## VII. SUMMARY AND CONCLUSION

In the present paper, we discuss a 2D FM with dipolar forces at $0 \leq T \ll T_C$ as described by the Hamiltonian (2) and consider the renormalization of the bare spin-wave spectrum (14) due to interaction between spin waves. For this purpose, we carry out a comprehensive analysis of the first $1/S$ corrections to the spin-wave spectrum originating from diagrams shown in Fig. 2.

We obtain the following results for $S \sim 1$. Corrections to the square of the real part of the spectrum are given by Eqs. (30) and (32). In particular, at $T \gg S\omega_0$, where $\omega_0$ is the characteristic dipolar energy given by Eq. (1), thermal corrections result simply in the renormalization (28) of the constants $D$ (spin-wave stiffness) and $\omega_0$ in the bare spectrum (14). This renormalization is small at $T \ll T_C$. However, it is significant that, similar to the 3D FM considered in our previous paper,[11] we also obtain the spin-wave gap $\Delta$ in the spectrum given by Eq. (31). This gap stemming from the spin-wave interaction greatly renormalizes the bare gapless spectrum (14) at $k \lesssim (\Delta/S\omega_0)^2$ (see Fig. 3).

Spin-wave damping $\Gamma_{\mathbf{k}}$ at $T=0$ is given by Eqs. (34) and (36) for momenta $1 \gg k \gg \sqrt{S\omega_0/D}$ and $k \ll \sqrt{S\omega_0/D}$, respectively. There is a region in the $\mathbf{k}$ space at small momenta sketched in Fig. 4 in which the damping is equal to zero. In the meantime, we find a great thermal enhancement of the damping in this region.

Temperature fluctuations give the main contribution to the spin-wave damping at $T \gg S\omega_0$, which is given by Eqs. (34), (36), (48), and (49) for momenta $k \gg \sqrt{S\omega_0/D}$, $S\omega_0/D \ll k \ll \sqrt{S\omega_0/D}$, $\Delta/\sqrt{TD} \lesssim k \ll S\omega_0/D$, and $k < \Delta/\sqrt{TD}$, respectively. The dependence of the damping on the momentum is sketched in Fig. 5 for $k \ll 1$. It is seen that $\Gamma_{\mathbf{k}}$ is highly anisotropic at $k \gtrsim S\omega_0/D$. The damping increases with decreasing $k$ up to $k \sim \Delta/\sqrt{TD}$ if $\mathbf{k}$ is directed along a square edge (i.e., if $|\sin 2\phi_{\mathbf{k}}|=0$). In contrast, the damping is not a monotonic function of $k$ when $|\sin 2\phi_{\mathbf{k}}| \sim 1$: it decreases with decreasing $k$ up to $k \sim (S\omega_0/D)^{2/3}$ and then it rises up to $k \sim \Delta/\sqrt{TD}$. The damping is only slightly anisotropic in the interval $\Delta/\sqrt{TD} \lesssim k \lesssim S\omega_0/D$. There is a peak at $k \sim \Delta/\sqrt{TD}$ at any given $\phi_{\mathbf{k}}$, the height of which can be estimated by using Eq. (48). If the temperature is large enough so that the interval is finite, which is given by $(\Delta/S\omega_0)^2 \gg k \gtrsim \Delta/\sqrt{TD}$, the peak height is given by Eq. (50). This peak is followed by an exponential decay of the damping at $k < \Delta/\sqrt{TD}$ having the form (49).

An important quantity to be examined is the ratio of the spin-wave damping and the real part of the spectrum $\Gamma_{\mathbf{k}}/\epsilon_{\mathbf{k}}$, which is much smaller than unity if magnons are well-defined quasiparticles. It is seen from Eqs. (34), (36), and (48) that the ratio $\Gamma_{\mathbf{k}}/\epsilon_{\mathbf{k}}$ rises upon decreasing $k$ at $k \gtrsim S\omega_0/D$ for all $\phi_{\mathbf{k}}$. This growth changes into exponential decay at $k \lesssim \Delta/\sqrt{TD}$ given by Eq. (49). Then, there is a peak in $\Gamma_{\mathbf{k}}/\epsilon_{\mathbf{k}}$ at $k \sim \Delta/\sqrt{TD}$ and at any given $\phi_{\mathbf{k}}$. This peak rises and its position moves to a smaller $k$ as $S$ increases at a given ratio $T/T_C$ or as $T$ increases at a given $S$ (see Fig. 6). In the meantime, its height is restricted by Eq. (50), which is proportional to $T/D$. In the case of $S \sim 1$, we have $T/D \ll 1$ when $T \ll T_C$.

On the other hand, as pointed out in Sec. IV C, the temperature can be greater than $D$ for large spin values much greater than unity, $S \gtrsim \ln\{4\pi S[D/(S\omega_0)]^{3/2}\}$, such that $D < T \ll T_C \propto DS$. The renormalization of the spectrum should be reconsidered at such large $T$ and $S$ because additional large temperature $1/S$ corrections arise. Such reconsideration is carried out in Sec. V. In particular, we find the thermal renormalization (28) of the constants $D$ and $\omega_0$ in the bare spectrum (14), where $W(T)$ and $V(T)$ are given by Eq. (56) in this case. Then the thermal correction to the gap becomes important and we have Eq. (55) for the gap at $T \sim D$, which transforms into Eq. (57) at $2SJ_0 \ll T \ll T_C$, where $2SJ_0$ is the spin-wave bandwidth. By focusing on the spin-wave damping renormalization at small $k$ only, we observe that the peak height of $\Gamma_{\mathbf{k}}/\epsilon_{\mathbf{k}}$ cannot exceed the value given by Eq. (59), which is approximately equal to 0.16 for the simple square lattice and is a counterpart of Eq. (50) for $S \sim 1$. It is interesting to note the numerical smallness of the peak height in $\Gamma_{\mathbf{k}}/\epsilon_{\mathbf{k}}$ when $S \gg 1$ and $T_C \gg T \gg 2SJ_0$ that is contrary to the case of small $S$, in which the peak in $\Gamma_{\mathbf{k}}/\epsilon_{\mathbf{k}}$ cannot exceed the value (50) proportional to $T/D \ll 1$. The small value given by Eq. (59) only slightly increases upon taking into account a frustrating next-nearest-neighbor exchange coupling (see Fig. 7). The limiting case of classical spins is also discussed in Sec. V at $T \ll j$, where $j$ is the exchange constant in the classical model [see Eq. (61)]. We obtain expression (62) for the gap and the peak in $\Gamma_{\mathbf{k}}/\epsilon_{\mathbf{k}}$ at $k=0$, the height of which is *precisely* given by Eq. (59) (see Fig. 6). Thus, we find that *magnons are well-defined quasiparticles* in both quantum and classical 2D FMs with dipolar forces.

We note that the appearance of the gap is accompanied by the anisotropy in the total energy of the quantum 2D FM given by Eq. (20) and caused by quantum fluctuations lifting the degeneracy of the classical ground state. We demonstrate in Sec. VI the relation between the dipolar anisotropic term (20) in the total energy and the gap in the spectrum at $T=0$.

Spin Green's functions $\chi_{ij}(\omega,\mathbf{k})$ are derived in Sec. VI with the results (67) and (68) for the transverse diagonal components $\chi_{xx}(\omega,\mathbf{k})$ and $\chi_{yy}(\omega,\mathbf{k})$, and Eqs. (69) and (70)

for the uniform longitudinal one $\chi_{zz}(\omega,\mathbf{0})$. It should be noted that if one did not take into account the spin-wave gap the infrared singularity would appear in the form $\mathrm{Im}\,\chi_{zz}(\omega\to 0,\mathbf{0})\sim\omega^{-3/2}$. Such a singularity is a nonphysical one, since it leads to an infinitely large absorption function $Q_\omega \propto \omega\,\mathrm{Im}\,\chi(\omega)$ at $\omega=0$. The spin-wave gap screens this singularity: as seen from Eq. (70), $\mathrm{Im}\,\chi_{zz}(\omega,\mathbf{0})=0$ at $\omega<2\Delta$.

A modification of the results by taking into consideration the easy-plane exchange anisotropy (71) is discussed briefly in Sec. VI. In particular, we have shown that expressions (31) and (57) for the gap should be multiplied by the factor $\sqrt{\tilde{\omega}_0/\omega_0}$, where $\tilde{\omega}_0$ is given by Eq. (72).

Expression (66) for the magnetization in 2D FM is obtained, which differs from the well-known result of Ref. 4. Higher order corrections to the spectrum are discussed in Sec. VI and it is concluded that they are small compared to the first corrections obtained.

In conclusion, we would like to note that the spectrum is gapless in 3D antiferromagnets with dipolar forces in the spin-wave approximation[33] and the spin-wave interaction should lead to the gap in 3D antiferromagnets similar to 2D and 3D FMs.

## ACKNOWLEDGMENTS

This work was supported by the Russian Science Support Foundation, President of Russian Federation (Grant No. MK-1056.2008.2), RFBR Grant No. 06-02-16702, and Russian Programs "Quantum Macrophysics," "Strongly correlated electrons in semiconductors, metals, superconductors and magnetic materials," and "Neutron Research of Solids."

## APPENDIX A: CALCULATION OF $\Omega^{(3)}(\omega,\mathbf{k})$

We present in this appendix some details of the calculation of $\Omega^{(3)}(\omega,\mathbf{k})$ that is a contribution to $\Omega(\omega,\mathbf{k})$ given by Eq. (18) from the loop diagram shown in Fig. 2(c). This diagram originates from $\mathcal{H}_3$ terms (10) in the Hamiltonian. As a result of simple calculations, we are led to the following quite cumbersome expressions:

$$\Omega^{(3)}(i\omega,\mathbf{k}) = -Dk^2\frac{S}{\mathfrak{N}}T\sum_{q_1+q_2=k}\frac{1}{[(i\omega_1)^2-\epsilon_1^2][(i\omega_2)^2-\epsilon_2^2]}$$
$$\times\{(Q_{\mathbf{k}}^{xz})^2(B_1B_2+E_1E_2+\omega_1\omega_2) \quad \text{(A1a)}$$
$$+2Q_{\mathbf{k}}^{xz}Q_1^{xz}[(E_1-B_1)(E_2-B_2)+\omega_1\omega_2] \quad \text{(A1b)}$$
$$+Q_1^{xz}Q_2^{xz}[(E_1-B_1)(E_2-B_2)-\omega_1\omega_2]$$
$$+2(Q_2^{xz})^2E_1(E_2-B_2)\} \quad \text{(A1c)}$$
$$-\frac{S^2\omega_0\alpha}{\mathfrak{N}}T\sum_{q_1+q_2=k}\frac{1}{[(i\omega_1)^2-\epsilon_1^2][(i\omega_2)^2-\epsilon_2^2]}$$
$$\times\{Q_1^{xz}(Q_1^{xz}+Q_2^{xz})(E_1-B_1)(E_2-B_2) \quad \text{(A1d)}$$
$$+(Q_{\mathbf{k}}^{xz})^2(B_1B_2+E_1E_2+\omega_1\omega_2) \quad \text{(A1e)}$$
$$+2Q_{\mathbf{k}}^{xz}Q_1^{xz}[(E_1-B_1)(E_2-B_2)+\omega_1\omega_2]\} \quad \text{(A1f)}$$
$$-i\omega\frac{2S}{\mathfrak{N}}T\sum_{q_1+q_2=k}\frac{i\omega_1}{[(i\omega_1)^2-\epsilon_1^2][(i\omega_2)^2-\epsilon_2^2]}$$
$$\times\{Q_2^{xz}(Q_1^{xz}+Q_2^{xz})(E_2-B_2) \quad \text{(A1g)}$$
$$-Q_{\mathbf{k}}^{xz}[Q_1^{xz}(E_2+B_2)+Q_2^{xz}(B_2-E_2)]\}, \quad \text{(A1h)}$$

where $k=(\mathbf{k},\omega)$, $q_{1,2}=(\mathbf{q}_{1,2},\omega_{1,2})$, and we drop the index $\mathbf{q}$ in Eqs. (A1a)–(A1h) to lighten the notation. Sums $\Sigma+\bar{\Sigma}$ and $\Sigma+\bar{\Sigma}+\Pi+\Pi^\dagger$ lead to terms (A1a)–(A1f), respectively, whereas terms (A1g) and (A1h) result from $i\omega(\Sigma-\bar{\Sigma})$ [see Eq. (18)].

One obtains the following expressions after a summation over imaginary frequencies and analytical continuation on $\omega$ from an imaginary axis to the real one:

$$T\sum_{\omega_1}\frac{1}{[(i\omega_1)^2-\epsilon_1^2][(i\omega_1-i\omega)^2-\epsilon_2^2]}$$
$$=\frac{1+2N(\epsilon_1)}{2\epsilon_1[(\epsilon_1+\epsilon_2)^2-(\omega+i\delta)^2]}+\frac{1+2N(\epsilon_2)}{2\epsilon_2[(\epsilon_1+\epsilon_2)^2-(\omega+i\delta)^2]}$$
$$+\frac{2(\epsilon_1-\epsilon_2)[N(\epsilon_2)-N(\epsilon_1)]}{[(\epsilon_1+\epsilon_2)^2-(\omega+i\delta)^2][(\epsilon_1-\epsilon_2)^2-(\omega+i\delta)^2]}, \quad \text{(A2a)}$$

$$T\sum_{\omega_1}\frac{(i\omega_1)(i\omega-i\omega_1)}{[(i\omega_1)^2-\epsilon_1^2][(i\omega_1-i\omega)^2-\epsilon_2^2]}$$
$$=\frac{\epsilon_1[1+2N(\epsilon_1)]}{2[(\epsilon_1+\epsilon_2)^2-(\omega+i\delta)^2]}+\frac{\epsilon_2[1+2N(\epsilon_2)]}{2[(\epsilon_1+\epsilon_2)^2-(\omega+i\delta)^2]}$$
$$-\frac{2\epsilon_1\epsilon_2(\epsilon_1-\epsilon_2)[N(\epsilon_2)-N(\epsilon_1)]}{[(\epsilon_1+\epsilon_2)^2-(\omega+i\delta)^2][(\epsilon_1-\epsilon_2)^2-(\omega+i\delta)^2]}, \quad \text{(A2b)}$$

$$T\sum_{\omega_1}\frac{i\omega_1}{[(i\omega_1)^2-\epsilon_1^2][(i\omega_1-i\omega)^2-\epsilon_2^2]}$$
$$=\omega\left(\frac{1+2N(\epsilon_2)}{2\epsilon_2[(\epsilon_1+\epsilon_2)^2-(\omega+i\delta)^2]}\right.$$
$$\left.+\frac{2\epsilon_1[N(\epsilon_2)-N(\epsilon_1)]}{[(\epsilon_1+\epsilon_2)^2-(\omega+i\delta)^2][(\epsilon_1-\epsilon_2)^2-(\omega+i\delta)^2]}\right). \quad \text{(A2c)}$$

We now calculate the real part of $\Omega^{(3)}(\omega,\mathbf{k})$ by using Eqs. (A2a)–(A2c). Term (A1d) is the only term that remains finite at $\omega,\mathbf{k}=0$ and leads to the contribution (29) to the spin-wave gap and to the second term in the square brackets in Eq. (57). The rest of the corrections in Eqs. (A1a)–(A1h) are much smaller than either term (A1d) or corrections from the Hartree–Fock diagram given by Eqs. (24) and (25). Let us estimate them. Term (A1a) is of the order of $\omega_0^{3/2}k^{5/2}\sin^2 2\phi_{\mathbf{k}}(k\sqrt{\omega_0 D}+T)/\sqrt{D}$, $\omega_0^2k^2\sin^2 2\phi_{\mathbf{k}}(k\sqrt{S\omega_0/D}+T/D)$, and $\omega_0^2\sin^2 2\phi_{\mathbf{k}}(\omega_0^2+k^2TD)/D^2$ at $k\ll S\omega_0/D$, $S\omega_0/D\ll k\ll\sqrt{S\omega_0/D}$, and $k\gg\sqrt{S\omega_0/D}$, respectively. Term

(A1c) is of the order of $k^2\omega_0^2$. It is much smaller than the first term in Eq. (24) if $\ln(D/\omega_0)\gg 1$, which we assume to hold. Contributions (A1b) cannot give more than terms (A1a) and (A1c). Term (A1e) is of the order of $\omega_0^{5/2}\sqrt{k}\sin^2 2\phi_{\mathbf{k}}(k\sqrt{\omega_0 D}+T)/D^{3/2}$, $\omega_0^3\sin^2 2\phi_{\mathbf{k}}(k\sqrt{\omega_0 D}+T)/D^2$, and $\omega_0^3\sin^2 2\phi_{\mathbf{k}}(\omega_0^2/k^2+TD)/D^3$ at $k\ll S\omega_0/D$, $S\omega_0/D\ll k\ll\sqrt{S\omega_0/D}$, and $k\gg\sqrt{S\omega_0/D}$, respectively. Term (A1f) does not exceed term (A1e). Term (A1g) is of the order of $\omega^2(\omega_0^2/D^2)[\ln(D/\omega_0)+T/(\omega_0+Dk^2)]$. Term (A1h) does not exceed the sum of terms (A1b) and (A1f).

Let us turn now to the imaginary part of $\Omega^{(3)}(\omega,\mathbf{k})$. Corresponding calculations have been straightforwardly done by using Eqs. (A1a)–(A1h) with the following results.

$k\gg\sqrt{S\omega_0/D}$. Terms (A1c) and (A1g) give the main equal contributions at small temperature, which lead to $T$-independent terms in Eq. (34). Terms (A1c) and (A1g) give equal contributions to the last term in Eq. (34). The second term in the square brackets in Eq. (34) containing $f(\phi_{\mathbf{k}})$ originates from terms (A1a)–(A1c): endowments of terms (A1a) and (A1c) are equal and twice as little as that of term (A1b). The origin of the function $f(\phi_{\mathbf{k}})$ is the following. The sum of the form $\Re^{-1}\Sigma_{\mathbf{q}}\delta[\cos(\phi_{\mathbf{k}}-\phi_{\mathbf{q}})-\epsilon_{\mathbf{q}}/2Dkq]/q\epsilon_{\mathbf{q}}^2$ appears in the corresponding expressions, in which the summation over small momenta $q\ll S\omega_0/D$ is essential. We have for the square of the spectrum at such $\mathbf{q}$ [cf. Eq. (35)]

$$\epsilon_{\mathbf{q}}^2\approx\frac{\alpha(S\omega_0)^3}{4D}\left(\tilde{q}^2+\tilde{q}\sin^2\phi_{\mathbf{q}}+\frac{4D\Delta^2}{\alpha S^3\omega_0^3}\right), \tag{A3}$$

where $\tilde{q}=q2D/S\omega_0$.

$S\omega_0/D\ll k\ll\sqrt{S\omega_0/D}$. One finds Eq. (36) in this regime. The term in Eq. (36) containing $\mathcal{A}_{1,2,3}(\mathbf{q})$ comes from terms (A1d)–(A1f), whereas those containing $\mathcal{B}_1(\mathbf{k})$, $\mathcal{B}_2(\mathbf{k})$, and $\mathcal{B}_3(\mathbf{k})$ originate from terms (A1c), (A1g), and (A1d), respectively. The term in Eq. (36) that is proportional to $\mathcal{B}_4$ comes from terms (A1d)–(A1f).

We now demonstrate in what way the quantity $\mathcal{L}(q,\mathbf{k})$ appears in Eq. (34). When $S\omega_0/D\ll k\ll\sqrt{S\omega_0/D}$, it is not sufficient to use the leading term in the expression for the spectrum assuming that $\epsilon_{\mathbf{k}}\approx\sqrt{S\alpha\omega_0 D}k$. In reality, we have, in this case, $\delta(\epsilon_{\mathbf{k}}-\epsilon_{\mathbf{q}}-\epsilon_{\mathbf{k}+\mathbf{q}})\propto\delta((\phi_{\mathbf{k}}-\phi_{\mathbf{q}}-\pi)^2)$ and $\delta(\epsilon_{\mathbf{k}}-\epsilon_{\mathbf{q}}+\epsilon_{\mathbf{k}+\mathbf{q}})\propto\delta((\phi_{\mathbf{k}}-\phi_{\mathbf{q}})^2)$ if $S\omega_0/D\ll k,q,|\mathbf{k}+\mathbf{q}|\ll\sqrt{S\omega_0/D}$. At the same time, expressions under the sums do not vanish at $\phi_{\mathbf{q}}=\phi_{\mathbf{k}}$ or $\phi_{\mathbf{q}}=\phi_{\mathbf{k}}\pm\pi$. Then, the appearance of the squares in the arguments of delta functions signifies that one should take into account smaller terms in the expression for the spectrum, as follows:

$$\epsilon_{\mathbf{q}}\approx\sqrt{S\alpha\omega_0 D}\left(q+\frac{S\omega_0}{4D}\sin^2\phi_{\mathbf{q}}+\frac{Dq^3}{2\alpha S\omega_0}+\frac{\Delta^2}{2\alpha S\omega_0 Dq}\right). \tag{A4}$$

By using Eq. (A4), if $S\omega_0/D\ll k,q,|\mathbf{k}+\mathbf{q}|\ll\sqrt{S\omega_0/D}$, we have

$$\epsilon_{\mathbf{k}}-\epsilon_{\mathbf{q}}\pm\epsilon_{\mathbf{k}+\mathbf{q}}\approx-\frac{\sqrt{S\alpha\omega_0 D}}{2}\frac{k}{q(k-q)}\times\left[q_\perp^2-\frac{3Dk^4}{16\alpha S\omega_0}\mathcal{L}\left(2\frac{q}{k}-1,\mathbf{k}\right)\right], \tag{A5}$$

where $\mathbf{q}_\perp$ ($\mathbf{q}_\parallel$) is the component of $\mathbf{q}$ perpendicular (parallel) to $\mathbf{k}$. We assume in Eq. (A5) that $k-|q_\parallel|\pm|k+q_\parallel|=0$ and $q_\perp\ll q_\parallel,k$.

$k\ll S\omega_0/D$. In this regime, Im $\Omega^{(3)}(\omega,\mathbf{k})$ is finite only at high temperature and one has Eq. (48) for it. Term (A1d) only contributes to Eq. (48).

## APPENDIX B: DISCUSSION OF THE DISCREPANCY BETWEEN EQUATION (66) FOR THE MAGNETIZATION AND THE PREVIOUS RESULT

In this appendix, we comment on the discrepancy between Eq. (66) for the magnetization and the corresponding expression in Ref. 4. Equation (66) coincides with that obtained in Ref. 4 at $T\gg S\omega_0/\ln(D/[S\omega_0])$ and at $T=0$. In the meantime, a term was obtained in Ref. 4 that is proportional to $T^{3/2}\omega_0^{-7/4}$ at $T\ll\omega_0^{3/2}/\sqrt{J}$, which is much larger than the $T$-independent term in Eq. (66) at $\omega_0^{3/2}/\sqrt{J}\gg T\gg J(\omega_0/J)^{11/6}$. I believe that the term proportional to $T^{3/2}\omega_0^{-7/4}$ observed in Ref. 4 is an artifact. A careful calculation with the bare spectrum (14) gives the term proportional to $T^{3/2}\omega_0^{-3/4}$ rather than $T^{3/2}\omega_0^{-7/4}$ at $T\ll\omega_0^{3/2}/\sqrt{J}$, which is much smaller than the $T$-independent term. To confirm this finding, we note that the values of $(S-\langle S^z\rangle)/S$ obtained in the regimes of $T\gg\omega_0^{3/2}/\sqrt{J}$ and $T\ll\omega_0^{3/2}/\sqrt{J}$ should be of the same order at $T\sim\omega_0^{3/2}/\sqrt{J}$. At the same time, $T^{3/2}\omega_0^{-7/4}\sim\sqrt{\omega_0}$ and $T\ln(T/\omega_0^{3/2})\sim\omega_0^{3/2}$ at $T\sim\omega_0^{3/2}/\sqrt{J}$. Surprisingly, this artifact has not been revealed so far (see, e.g., Refs. 1 and 34). To conclude, one is led to the same expression (66) for $(S-\langle S^z\rangle)/S$ as a result of calculations using the bare (14) and renormalized spectra.

## APPENDIX C: EFFECT OF THE EXCHANGE ANISOTROPY

We briefly discuss in this appendix the effect of the exchange anisotropy given by Eq. (71). We consider here only the exchange anisotropy that differs from the on-site one, which has the form $A\Sigma_l(S_l^y)^2$ that exists in thin ferromagnetic films.[1] The reason is that it is technically easier to discuss the exchange anisotropy (71). Moreover, it is believed that these two types of anisotropies lead to similar physical results (see Ref. 2 and references therein). A more detailed discussion of the effect of the anisotropy in 2D FMs with dipolar forces will be published elsewhere. We consider below both signs of $A_{lm}$, i.e., both easy-axis and easy-plane anisotropies. Easy-axis anisotropy competes with the dipolar anisotropy, which favors in-plane spin alignment. We restrict ourselves here to the case of not too large easy-axis anisotropy, at which spins lie within the plane.

By adding $\mathcal{H}_a$ to the Hamiltonian (2), after the Dyson–Maleev transformation (8), one obtains a renormalization of

$E_{\mathbf{k}}$ and $B_{\mathbf{k}}$ in the bilinear part of the Hamiltonian (9) as follows:

$$E_{\mathbf{k}} \mapsto E_{\mathbf{k}} + \frac{SA_{\mathbf{k}}}{2}, \quad B_{\mathbf{k}} \mapsto B_{\mathbf{k}} - \frac{SA_{\mathbf{k}}}{2}, \tag{C1}$$

and a contribution to the four-magnon term,

$$\mathcal{H}_4^{(a)} = \frac{1}{4\mathfrak{N}} \sum_{\mathbf{k}_1+\mathbf{k}_2+\mathbf{k}_3+\mathbf{k}_4=0} A_2 a_{-1}^{\dagger}(a_2 - a_{-2}^{\dagger}) a_3 a_4. \tag{C2}$$

As a result of the renormalization (C1), at $k \ll 1$ [cf. Eq. (14)], the bare spectrum has the form

$$\epsilon_{\mathbf{k}}^{(a)} = \sqrt{(Dk^2 + S\tilde{\omega}_0\alpha)\left(Dk^2 + \frac{S\omega_0}{2}k\,\sin^2\phi_{\mathbf{k}}\right)}, \tag{C3}$$

where $\tilde{\omega}_0$ is given by Eq. (72). Notice that in the case of easy-axis anisotropy ($A<0$), the spectrum $\epsilon_{\mathbf{k}}^{(a)}$ becomes imaginary at small enough $k$ if $\tilde{\omega}_0 < 0$. At the same time, the in-plane spin alignment becomes energetically unfavorable if the anisotropy is as large as $\tilde{\omega}_0 \leq 0$. We imply below that $\tilde{\omega}_0 \sim \omega_0$ for $A<0$.

One is led to the following results after the corresponding calculations. Two regimes should be considered in this case: $T \ll S\tilde{\omega}_0$ and $T \gg S\tilde{\omega}_0$. At $T \ll S\tilde{\omega}_0$, for Re $\Omega(\omega, \mathbf{k})$, we have expression (30), which should be multiplied by $\tilde{\omega}_0/\omega_0$. As a result, the spin-wave gap has the form

$$\Delta^{(a)} = \sqrt{\alpha C S^2 \frac{\tilde{\omega}_0 \omega_0^2}{D}}, \tag{C4}$$

i.e., one is led to Eq. (31) multiplied by $\sqrt{\tilde{\omega}_0/\omega_0}$. At $T \gg S\tilde{\omega}_0$, we obtain Eq. (32), in which the last two terms should be multiplied by $\tilde{\omega}_0/\omega_0$. In the case of large $S$ and $T$ discussed in Sec. V, for the spin-wave gap, we have expression (57) multiplied by $\sqrt{\tilde{\omega}_0/\omega_0}$.

*syromyat@thd.pnpi.spb.ru


[1] K. De'Bell, A. B. MacIsaac, and J. P. Whitehead, Rev. Mod. Phys. **72**, 225 (2000).
[2] P. J. Jensen and K. H. Bennemann, Surf. Sci. Rep. **61**, 129 (2007).
[3] N. D. Mermin and H. Wagner, Phys. Rev. Lett. **17**, 1133 (1966).
[4] S. V. Maleev, Sov. Phys. JETP **43**, 1240 (1976).
[5] C. Pich and F. Schwabl, Phys. Rev. B **47**, 7957 (1993).
[6] B. P. Toperverg and A. G. Yashenkin, Phys. Rev. B **48**, 16505 (1993).
[7] T. S. Rahman and D. L. Mills, Phys. Rev. B **20**, 1173 (1979).
[8] A. I. Akhiezer, V. G. Bar'yakhtar, and S. V. Peletminskii, *Spin Waves* (North-Holland, Amsterdam, 1968).
[9] A. Kashuba, A. Abanov, and V. L. Pokrovsky, Phys. Rev. Lett. **77**, 2554 (1996).
[10] A. Abanov, A. Kashuba, and V. L. Pokrovsky, Phys. Rev. B **56**, 3181 (1997).
[11] A. V. Syromyatnikov, Phys. Rev. B **74**, 014435 (2006).
[12] J. R. Tessman, Phys. Rev. **96**, 1192 (1954).
[13] J. H. van Vleck, Phys. Rev. **52**, 1178 (1937).
[14] F. Keffer and T. Oguchi, Phys. Rev. **117**, 718 (1960).
[15] F. Keffer, *Handbook of Physics* (Springer, Berlin, 1966), Vol. 18, Pt. 2.
[16] M. Dantziger, B. Glinsmann, S. Scheffler, B. Zimmermann, and P. J. Jensen, Phys. Rev. B **66**, 094416 (2002).
[17] C. L. Henley, Phys. Rev. Lett. **62**, 2056 (1989).
[18] J. Villain, R. Bidaux, J. P. Carton, and R. Conte, J. Phys. (Paris) **41**, 1263 (1980).
[19] S. Prakash and C. L. Henley, Phys. Rev. B **42**, 6574 (1990).
[20] K. De'Bell, A. B. MacIsaac, I. N. Booth, and J. P. Whitehead, Phys. Rev. B **55**, 15108 (1997).
[21] A. Carbognani, E. Rastelli, S. Regina, and A. Tassi, Phys. Rev. B **62**, 1015 (2000).
[22] R. N. Costa Filho, M. G. Cottam, and G. A. Farias, Phys. Rev. B **62**, 6545 (2000).
[23] F. Dyson, Phys. Rev. **102**, 1217 (1956).
[24] F. Dyson, Phys. Rev. **102**, 1230 (1956).
[25] S. V. Maleev, Sov. Phys. JETP **6**, 776 (1958).
[26] M. H. Cohen and F. Keffer, Phys. Rev. **99**, 1128 (1955).
[27] Thermal corrections to the gap proportional to $\omega_0^3 T \ln[T/(S\omega_0)]/D^2$ from the Hartree–Fock diagram and from the loop diagram discussed in Sec. III B cancel each other. As a result, the thermal correction to the square of the gap for $S \sim 1$ is much smaller, $\omega_0^3 T^{3/2}/D^{5/2}$ (see discussion in Sec. III C). To find it, one should take into account $\mathcal{O}(k^2)$ corrections in the expansion of the dipolar tensor $Q_{\mathbf{k}}^{\rho\beta}$, which depend on the lattice type.
[28] Although $T_C$ given by Eq. (51) can differ several times from the real value of the Curie temperature (Ref. 34), this precision is sufficient for our estimations.
[29] Notice that even at large enough dipolar characteristic energy $\omega_0$ (remains small as compared to the exchange value), say, at $\omega_0 \approx 0.1J$, we have $S \gtrsim \ln\{4\pi S(D/[S\omega_0])^{3/2}\}$ only for pretty large spins $S \gtrsim 8$.
[30] A. B. Harris, D. Kumar, B. I. Halperin, and P. C. Hohenberg, Phys. Rev. B **3**, 961 (1971).
[31] P. D. Loly, 07281Ann. Phys. (N.Y.) **56**, 40 (1970).
[32] L. D. Landau and E. M. Lifshitz, *Statistical Physics*, 3rd ed., Landau and Lifshitz Course of Theoretical Physics Vol. 5 (Butterworth-Heinemann, Oxford, 1980), Pt. 1.
[33] A. B. Harris, Phys. Rev. **143**, 353 (1966).
[34] A. Grechnev, V. Y. Irkhin, M. I. Katsnelson, and O. Eriksson, Phys. Rev. B **71**, 024427 (2005).